ΑΛΕΞΑΝΔΡΕΙΟ ΤΕΧΝΟΛΟΓΙΚΟ ΕΚΠΑΙΔΕΥΤΙΚΟ ΙΔΡΥΜΑ ΘΕΣΣΑΛΟΝΙΚΗΣ

ΣΧΟΛΗ ΕΠΑΓΓΕΛΜΑΤΩΝ ΥΓΕΙΑΣ ΚΑΙ ΠΡΟΝΟΙΑΣ
ΤΜΗΜΑ ΙΑΤΡΙΚΩΝ ΕΡΓΑΣΤΗΡΙΩΝ

ROLE OF A MUSCLE-SPECIFIC E3 UBIQUITIN LIGASE: A NOVEL MUSCLE MASS REGULATOR.

ΠΤΥΧΙΑΚΗ ΕΡΓΑΣΙΑ

της

ΤΖΩΡΤΖΙΑΝΑ ΠΑΝΤΣΙ

Επιβλέπουσα: Δρ Παπουτσή Ανδρονίκη, Αναπληρώτρια Καθηγήτρια Βιολογίας-Γενετικής

Σε συνεργασία: Department Of Biomedical Sciences, University of Padova, Italy

Επιβλέπουσα: Vanina Romanello

2017

Acknowledgements

This thesis could not have been completed without the great support that I have received from so many people over the last one year. I wish to offer my most heartfelt thanks to the following people.

To my advisors and supervisors: Vanina Romanello, firstly, for giving me the opportunity to work in her laboratory and furthermore for the advice, support, and willingness that allowed me to discover the topic of science which I am truly passionate. Androniki Papoutsi, for the understanding, patience and the support although the difficult circumstances. I see in both of you the same drive and passion in your own work efforts, and I thank you for letting me do the same.

The Principal investigator: Marco Sandri., My colleagues, very close friends and family for six months: Giulia Favaro, Andrea Armani, Anaïs Franco, Martina Baraldo, Leonardo Nogara and Caterina Tezze.

My family for all the support from day one and the enormous encouragement that they give me all this time.

Thank you all.

Ευχαριστίες

Η πτυχιακή αυτη εργασία δεν θα μπορουσε ποτέ να ολοκληροθεί απουσία της υποστήρηξης που έλαβα απο τόσους πολλούς ανθρώπους τους τελευταίους έξι μήνες. Θα ήθελα, λοιπόν να ευχαριστήσω απο τα βάθη της καρδιάς μου στους ακόλουθους.

Την καθηγήτρια Vanina Romanello, αρχικά για την ευκαιρία που μου έδωσε να εργαστώ με το εργαστηριο της και επίσης, για τις συμβουλές, την υποστήριξη και την προθυμία που μου επέτρψαν αν ανακαλύψω τον τομέα της επιστήμης με τον οποίο επιθυμώ πραγματικά να ασχοληθώ. Την καθηγήτρια Ανδρονίκη Παπουτσή και την κατανόηση, την υπομονή και την υποστήριξη παρόλο τις δύσκολες συνθήκες. Βλέπω και στις δυο σας την ίδια παρακίνηση και πάθος στις δικές σας προσπάθειες και σας ευχαριστώ που με αφήσατε να το κάνω το ίδιο.

Τον κύριο ερευνητή (P.I): Marco Sandri. Τους συναδέλφους, πολυ καλούς φίλους και οικογένια μου για εξι μήνες: Giulia Favaro, Andrea Armani, Anaïs Franco, Martina Baraldo, Leonardo Nogara και Caterina Tezze.

Την οικογένια μου για την όλη υποστήριξη από την πρώτη στιγμή και την ενθάρινση όλο αυτό το διάστημα.Σας ευχαριστώ όλους θερμά.

Table of Contents

Preface

The skeletal muscle accounts for almost 40% of total body mass and represents a major site of metabolic activity. Skeletal muscle is a dynamic tissue: exercise and hormonal stimulation lead to an increase in protein synthesis and fiber size, a process called hypertrophy. Conversely, the loss of muscle mass, named atrophy, is the result of an increase in protein degradation. Muscle atrophy can occur in several pathological conditions like cancer, diabetes, chronic heart failure, AIDS, and during aging.

Atrophy is an active process controlled by specific signaling pathways and transcriptional programs but the identification of the precise signaling cascades that direct muscle wasting remains poorly understood. The Ubiquitin Proteasome System (UPS) is one of the major mechanisms that control proteolysis and ubiquitination of protein substrates. The specificity of ubiquitin-dependent degradation derives from many E3s that recognize specific substrates. This work is interested in the study of the role of Asb2β in vivo, a new E3 muscle-specific ubiquitin ligase. To understand its role, we generated skeletal muscle specific knock-out mouse models and we analyzed its function in physiological and in muscle wasting conditions.

Furthermore, characterization of different E3s and their respective substrates in skeletal muscle could represent an important step to understand the mechanisms that control muscle mass loss and, moreover, to develop targets for pharmacological intervention in muscle disease.

Πρόλογος

Ο σκελετικός μυς αντιπροσωπεύει σχεδόν το 40% της συνολικής μάζας σώματος και έχει έντονη μεταβολική δραστηριότητα. Ο σκελετικός μυς είναι ένας δυναμικός ιστός: η άσκηση και η ορμονική διέγερση οδηγούν σε αύξηση της πρωτεϊνοσύνθεσης και του μεγέθους των ινών, μια διαδικασία που ονομάζεται υπερτροφία. Αντιστρόφως, η απώλεια μυϊκής μάζας, που ονομάζεται ατροφία, είναι το αποτέλεσμα της αύξησης της αποικοδόμισης των πρωτεΐνης. Η ατροφία των μυών μπορεί να εμφανιστεί σε διάφορες παθολογικές καταστάσεις όπως ο καρκίνος, ο διαβήτης, η χρόνια καρδιακή ανεπάρκεια, το AIDS και κατά τη διάρκεια της γήρανσης.

Η ατροφία είναι μια ενεργή διαδικασία που ελέγχεται από συγκεκριμένες διαδρομές σηματοδότησης και μεταγραφικά προγράμματα, αλλά η ταυτοποίηση των ακριβών σηματοδοτικών καταρρακτών που οδηγούν στην απώλεια μυών παραμένει ελάχιστα κατανοητή. Το Πρωτεινικό Σύστημα Ουβικιτίνης (Ubiquitin Proteasome System UPS) είναι ένας από τους κύριους μηχανισμούς που ελέγχουν την πρωτεόλυση και την ουβικιτίνη των υποστρωμάτων των πρωτεϊνών. Η εξειδίκευση της εξαρτώμενης από την ουβικιτίνη αποικοδόμιση προέρχεται από πολλές E3 λιγάσες που αναγνωρίζουν συγκεκριμένα υποστρώματα. Η ερασλια αυτή στρέφει το ενδιαφέρον της στη μελέτη του ρόλου της Asb2β, μιας νέας λιποπρωτεΐνης της ουμπικουϊτίνης ειδικής για το μυ. Για να κατανοήσουμε το ρόλο της, δημιουργήσαμε ζωϊκά μοντέλα (ποντίκια) όπου το γονίδιο της Asb2β είναι διεγραμένο και αναλύσαμε τη λειτουργία του σε φυσιολογικές συνθήκες και συνθήκες μυϊκής ατροφίας.

Επιπλέον, ο χαρακτηρισμός και η περετέρο μελέτη των διαφόρων E3 λιγασών και των αντίστοιχων υποστρωμάτων τους στον σκελετικό μυ, θα μπορούσε να αποτελέσει ένα σημαντικό βήμα για την κατανόηση των μηχανισμών που ελέγχουν την απώλεια της μυϊκής μάζας και, επιπλέον, για την ανάπτυξη στόχων για φαρμακολογική επέμβαση στις νόσους που προσβάλουν τον μύ.

1 THEORITICAL PART

1.1 SKELETAL MUSCLE

1.1.1 STRUCTURE AND FUNCTION

In humans, skeletal muscle comprises approximately 40% of total body weight and contains 50–75% of all body proteins. Skeletal muscle is one of the most dynamic and plastic tissues of the human body. Muscle is composed by multinucleated, elongated and cylindrical cells called muscle fibers that run parallel to each other within a muscle. These cells are incredibly large, with diameter of up to 100μm and length of up to 30 cm. Muscles fibers are organized in bundles and separated by specific membrane system. Each muscle is surrounded by a connective

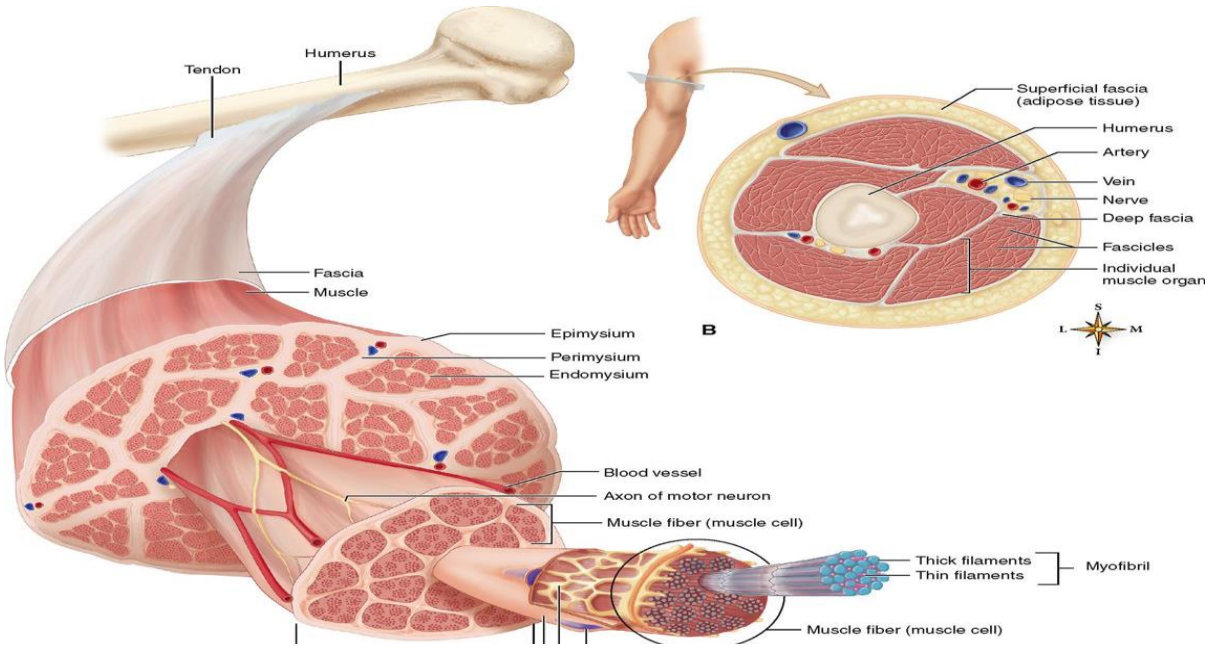

Image1: Schematic representation of muscle structure. (biology-forums.com)

tissue membrane called epimysium. Each bundle of muscle fiber is called fasciculus and is surrounded by a layer of connective tissue, called perimysium. Within the fasciculus, each individual muscle fiber is surrounded by connective tissue called endomysium.[1]

Skeletal muscle fibers (cells: myofibers) are long and narrow cells. The cytoplasm of skeletal muscle fibers is called sarcoplasm. Most of the sarcoplasm is occupied by

myofibrils, which are cylindrical bundles of contractile proteins. Each myofibril extends the length of a fiber and measures approximately 1 to 2 μm in diameter and contains repeating subunits that they are sarcomeres. Each of them has two primary components thin filaments (each of which contains two strands of actin and a single strand of regulatory protein) and thick filaments made of myosin. Movement of these two filaments relative to one another causes the lengthening and shortening of the sarcomere.[1]

Each individual sarcomere is flanked by dense protein discs called Z lines, which hold the myofilaments in place. The recurring sarcomeres produce a striated (striped) pattern along the length of the skeletal muscle fibers. The A band is the region where thick filaments are present, but the H zone is the region where only thick filaments are present. The thick filaments are composed of myosin. So the A band represents the whole length, of the myosin filament, which is composed of interwoven myosin molcules. Each myosin molecule within the myosin filament has a head and a tail. The heads are the bulbous elements that can be seen in the illustration. The I bands are the two regions where thin filaments exclusively are present. The Z lines, or Z disks, which have a jagged appearance under a microscope, are the boundaries between adjacent sarcomeres. The I bands span on either side of the Z-disks and represents the region between the ends of the thick filaments, that is, between the A

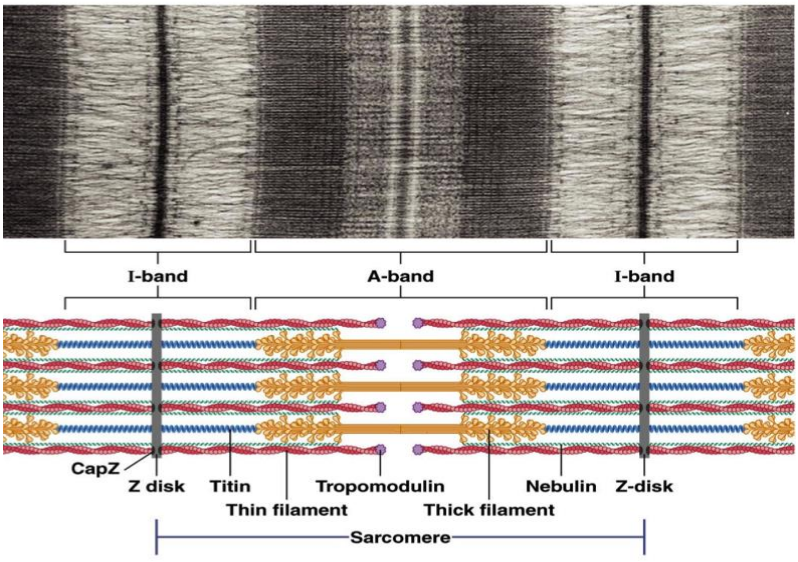

Image 2: Schematic and telescopical imaging of sarcomeres structure. (researchgate.net)

bands. In the I bands only actin is found (so remember the i in actin). (Image:2).

The division lying half way between the Z lines is known as the M line, where M stands for "middle." The M line corresponds to the region where strands of a protein called myomesin are found. During muscle contraction the thick filaments quickly slide along the thin filaments to shorten the myofibrils. The myofilaments themselves, however, do not contract. This muscle contraction is due to the excitation-contraction coupling, by which an electrical stimulus is converted into mechanical contraction. The general scheme is that an action potential arrives to depolarize the cell membrane. By mechanisms specific to the muscle type, this depolarization results in an increase in cytosolic calcium that is called a calcium transient. This increase in calcium activates calcium-sensitive contractile proteins that then use ATP to cause cell shortening. Concerning skeletal muscle, upon contraction, the A-bands do not change their length, whereas the I bands and the H-zone shorten. This is called the sliding filament hypothesis, which is now widely accepted. There are projections from the thick filaments, called cross-bridges which contain the part (head) of myosin linked to actin. Myosin head is able to hydrolyse ATP and covering chemical energy into mechanical energy.

To allow the simultaneous contraction of all sarcomeres, the sarcolemma penetrates into the cytoplasm of the muscle cell between myofibrils, forming membranous tubules called transverse tubules (T-tubules). The T-tubules are electrically coupled with the terminal cisternae which continue into the sarcoplasmic reticulum. Thus the Sarcoplasmic Reticulum, which is the enlargement of smooth.Endoplasmic Reticulum (ER) and which contains the majority of calcium ions required for contraction, extends from both sides of Ttubules into the myofibrils.[1]

Anatomically, the structure formed by T-tubules surrounded by two smooth ER cisternae is called the triad and it allows the transmission of membrane depolarization from the sarcolemma to the ER. The contraction starts when an action potential diffuses from the motor neuron to the sarcolemma and then it travels along T-tubules until it reaches the sarcoplasmic reticulum. Here the action potential changes the permeability of the sarcoplasmic reticulum, allowing the flow of calcium ions into the cytosol between the myofibrils. The release of calcium ions induces the myosin heads to interact with the actin, allowing the muscle contraction. The

contraction process is ATPdependent. The energy is provided by mitochondria which are located closed to Z line.[1]

The muscle fibers of mammalins are divided into two distinct classes: type I, also called slow fibres, and type II, called fast fibres. This classification considers only the mechanical properties. However the different fibre types also show peculiar features such as for example myosin ATPase enzymes, metabolism (oxidative or glycolytic), mitochondrial content revealed by succinate dehydrogenase (SDH) staining, and resistance to fatigue [2], [3]. It is possible to distinguish four major fibre types called I, IIA, IIX and IIB, based on the presence of different myosin heavy chain (MyHC) isoforms [4]. Fibres type I express the slow isoform MyHC-1 coded by MYH7 gene, and show a great content of mitochondria, high levels of myoglobin, high capillary density and oxidative capacity. For these reasons muscles containing many type I fibres appear red. Type IIA fibres express MyHC-2A, coded by MYH2 gene. IIA myofibers are slower compared to type I, but faster than type IIX and IIB, and they exhibit an oxidative metabolism and a relative fatigue-resistance due to the rich mitochondria content [5],[6]. Given all these characteristics, IIA fibres are also termed fast oxidative fibres. The IIX fiber type, expressing MyHC-2X, and IIB fibre type, which expresses MyHC-2B, are called fast-glycolytic fibres and show a prominent glycolytic metabolism containing few mitochondria of small size, high myosin ATPase activity, the fastest rate of contraction and the highest level of fatigability.

The fibre-type profile of different muscles is initially established during development independently of neural influence, but nerve activity has a major role in the maintenance and modulation of its properties in adult muscle. Indeed during postnatal development and regeneration, a default nerve activity-independent pathway of muscle fibre differentiation, which is controlled by thyroid hormone, leads to the activation of a fast gene program. On the contrary, the post-natal induction and maintenance of the slow gene program is dependent on slow motoneuron activity. The muscle fibre-type then undergoes further changes during postnatal life, for example fibre-type switching could be induced in adult skeletal muscles by changes in nerve activity. [7]

1.2 MUSCLE HYPERTROPHY AND ATROPHY

The regulation of the muscle mass depends on protein degradation and protein synthesis which are completely effected by the physical activity, hormones and diseases. Muscle growth is mainly due to protein synthesis, that, when exceeds, leads to muscle hypertrophy. On the contrary, loss of proteins, organelles and cytoplasm are major causes of muscle atrophy.

1.2.1 MUSCLE HYPERTROPHY

Muscle hypertrophy involves an increase in size of skeletal muscle through a growth in size of its component cells. Two factors contribute to hypertrophy: sarcoplasmic hypertrophy, which focuses more on increased muscle glycogen storage and myofibrillar hypertrophy, which focuses more on increased myofibril size.

Protein turnover is mainly regulated by a highly conserved pathway composed of the insulin-like growth factor IGF-1 and a cascade of intracellular effectors that include the kinases Akt/PKB and mTOR. Muscle-specific IGF-1 overexpression results in muscle hypertrophy and, importantly, the growth of muscle mass matches with a physiological increase of muscle strength. Furthermore, the overexpression of a constitutively active form of Akt in adult skeletal muscle induced muscle hypertrophy, this pathway promotes muscle growth and blocks protein degradation [8]. Akt pathway, in fact, controls in an opposite manner two important downstream

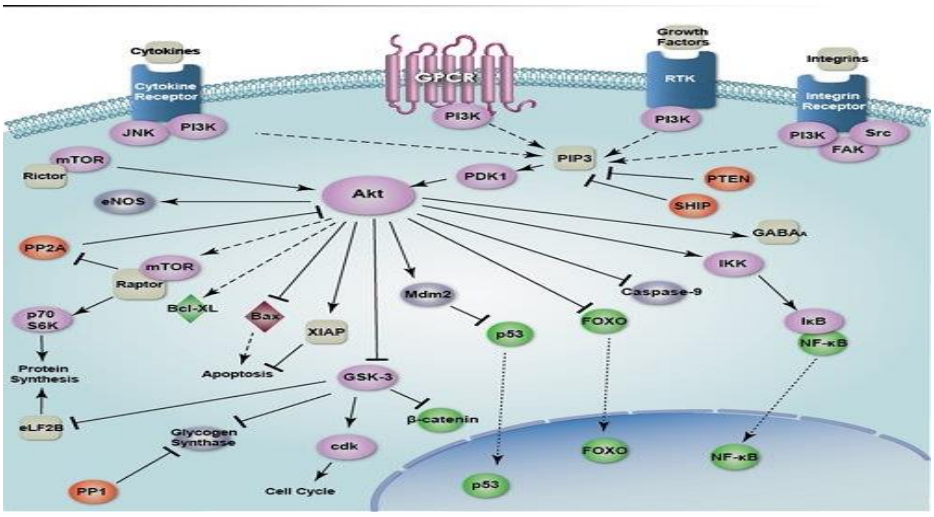

Image 3: Schematic imaging of AKT signaling pathway. (From AntiSel - A. Selidis Bros SA)

targets: mammalian target of rapamycin (mTOR) and glycogen synthase kinase 3 beta (GSK3β). In the first case, Akt phosphorylates and activates the serine/threonine protein kinase mTOR, a master regulator of cell growth mTOR promotes protein synthesis through the activation of the ribosomal protein S6 kinases 1 and 2 (S6K1 and S6K2) and blocking the inhibition of the initiation factor 4E binding protein 1 (4EBP1). In the other case, the inhibition of GSK3β from Akt stimulates proteins synthesis, since GSK3β normally blocks protein translation initiated by eIF2B protein (Glass, 2005). In conclusion, IGF-1- Akt axis is a major mediator of skeletal muscle hypertrophy (Image:3). Recently, it has been reported that also myostatin and other members of the TGF-β pathway contribute to regulation of muscle mass in adulthood [9],[10]. TGF-β pathway has a negative effect on muscle growth mediated by Smad2 and Smad3 transcription factors. Moreover, bone morphogenetic protein (BMP) signaling, acting through Smad1, Smad5 and Smad8 (Smad1/5/8), is one of the fundamental hypertrophic signals in mice. It has been demonstrated that when the BMP pathway is blocked or myostatin expression is increased, Smad4 binds to phosphorylated Smad2/3, leading to atrophy. On the contrary, a decrease in Smad2/3 phosphorylation levels, leads to the release of Smad4, which promotes hypertrophy through its binding to Smad1/5/8. Importantly, it has been identified a newly characterized ubiquitin-ligase, named MUSA1, as the molecular mechanism underlying the anti-atrophic action of the BMP pathway that has a negative effect on its expression. This work provided evidences that also BMP signaling is involved in the regulation of adult muscle mass in normal and pathological situations [10].

1.2.2 MUSCLE ATROPHY

Skeletal muscle atrophy attributable to muscular inactivity, diseases (like sepsis, cancer, diabetes, AIDS, heart and renal failure), denervation and during aging has significant adverse functional consequences. Decreases in protein synthesis and increases in protein degradation both have been shown to contribute to muscle protein loss due to disuse, and recent work has delineated elements of both synthetic and proteolytic processes underlying muscle atrophy. It is also becoming evident that interactions among known proteolytic pathways (ubiquitin-proteasome, autophagy-lysosomal, and calpain) are involved in muscle proteolysis during atrophy. Moreover,

a common set of genes, some which are groups of genes always modulated in several atrophying conditions were identified. These so “Atrogenes” are involved in protein degradation, protein synthesis, ROS detoxification, unfolded protein response (UPR), energy production and growth-related processes. [11]. Muscle atrophy involves the shrinkage of myofibers due to a net loss of proteins. The ubiquitin-proteasome system and the autophagy-lysosome pathway are the degradation systems involved in this process [12].

1.3 PROTEIN DEGRADATION SYSTEMS

There are several systems in the cell is necessary for the removal of proteins, aggregates and organelles. These systems are called protein degradation systems. The main proteolytic systems are the ubiquitin-proteasome system (UPS) and the autophagy lysosome system. The proteasome generally recognizes only ubiquitinated substrates witch are short live proteins. In contrast, degradation by lysosome is specific for long-lived proteins and in this case organelles and cytosolic components can be delivered to the lysosome by autophagy [13].

1.3.1 Autophagy-Lysosome System

Autophagic Lysosome System involves dynamic rearrangements of membranes which engulf a portion of cytoplasm for its degradation in the lysosome. The portion of cytoplasm, including excess or abnormal organelles is sequestered into

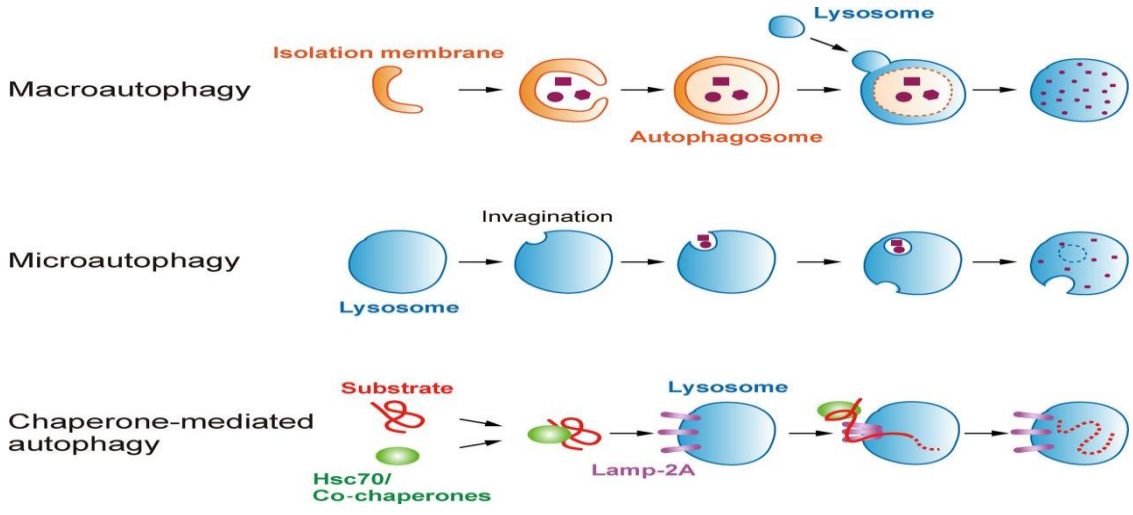

Image 4 : Schematic imagind of forms of autophagy: macroautophagy, microautophagy and CMA. (Organellophagy: Eliminating cellular building blocks via selective autophagy, Koji Okamoto, May 2014.)

double-membrane vesicles and delivered to the degradative organelle, the lysosome, for breakdown and for recycling the generated molecules.

This process has an important role in various biological events, such as adaptation to environmental changes, cellular remodeling during development and differentiation and ageing. Autophagy is also involved in preventing certain types of disease, like Parkinson and Huntington, although it may contribute to some pathologies. Autophagy is also constitutively active in skeletal muscle, as shown by the accumulation of autophagosomes seen in human myopathies, caused by genetic deficiency of lysosomal proteins (Pompe's and Danon's diseases), or by pharmacological inhibition of lysosomal function [14]. The generation of transgenic mice for LC3, the mammalian homolog of the essential autophagy gene Atg8, fused with GFP defined the amount of autophagy in different tissues and whether different organs respond to fasting by activating autophagosome formation [15].

Indeed, skeletal muscle has been found to be one of the tissues with the highest induction of autophagy [16]. In fast skeletal muscle of transgenic mice, food deprivation induced the rapid appearance of cytoplasmic fluorescent dots, corresponding to autophagosomes [16]. In different cell systems, autophagy is activated by depletion of nutrients or of growth factors and, according to current views, in most cases this is mediated by the kinase mTOR [17]. Autophagy is suppressed by mTOR, which is in turn controlled directly by the level of intracellular amino acids, by growth factors via Akt/PKB and by cell energy status via AMPK. Accordingly, rapamycin, a specific inhibitor of mTOR, activates autophagy. However, autophagy can also be induced by mTOR-independent mechanisms: leucine starvation has been reported to induce mTOR-independent autophagy in cultured myotubes [18], and mTOR has also been found to be dispensable in other cell systems [19],[20],[21]. Up regulation of autophagy and lysosomal genes has been documented at the transcript and protein level in different settings, but the mechanisms controlling this transcriptional regulation and their physiological relevance have not been characterized. The lysosomal proteinase cathepsin L is induced in muscle wasting [22], and microarray analyses suggest that this is also true for the autophagy-related genes LC3 and Gabarapl1 [23]. Several studies point to up regulation of autophagy genes in other cell systems and in different experimental conditions [24]. However,

the factors involved in the transcriptional regulation of autophagy genes have not yet been identified [25].

1.3.2 Ubiquitin-Proteasome System

In the ubiquitin –proteasome system, the 26S proteasome targets the proteins for degradation through the chain of ubiquitin molecules.

Ubiquitylation of protein substrates occurs through the sequential action of specific enzymes: a ubiquitin-activating enzyme E1, a ubiquitin-conjugating enzyme E2 and a ubiquitin ligase E3 responsible for the specific recognition of substrates through dedicated interaction domains [26]. More specifically, the targeting reaction begins with ubiquitin-activating enzyme (E1), that hydrolyzes ATP and adenylylates a ubiquitin molecule. This adenylylated ubiquitin is then transferred to a cysteine of a second enzyme, ubiquitin-conjugating enzyme (E2). At the end a member of a highly diverse class of enzymes known as ubiquitin ligases (E3) recognizes the specific protein to be ubiquitinated and catalyzes the transfer of ubiquitin from E2 to this target protein, the protein now is ubiquitinated. Once that happens, the protein is accosted to the proteasome to be degraded. The polybiquitin chain can be removed by the de-ubiquitinating enzymes.

The ubiquitin pathway, upon others, is responsible for the muscle protein degradation in normal or abnormal situations. The muscle mass loss can be caused by

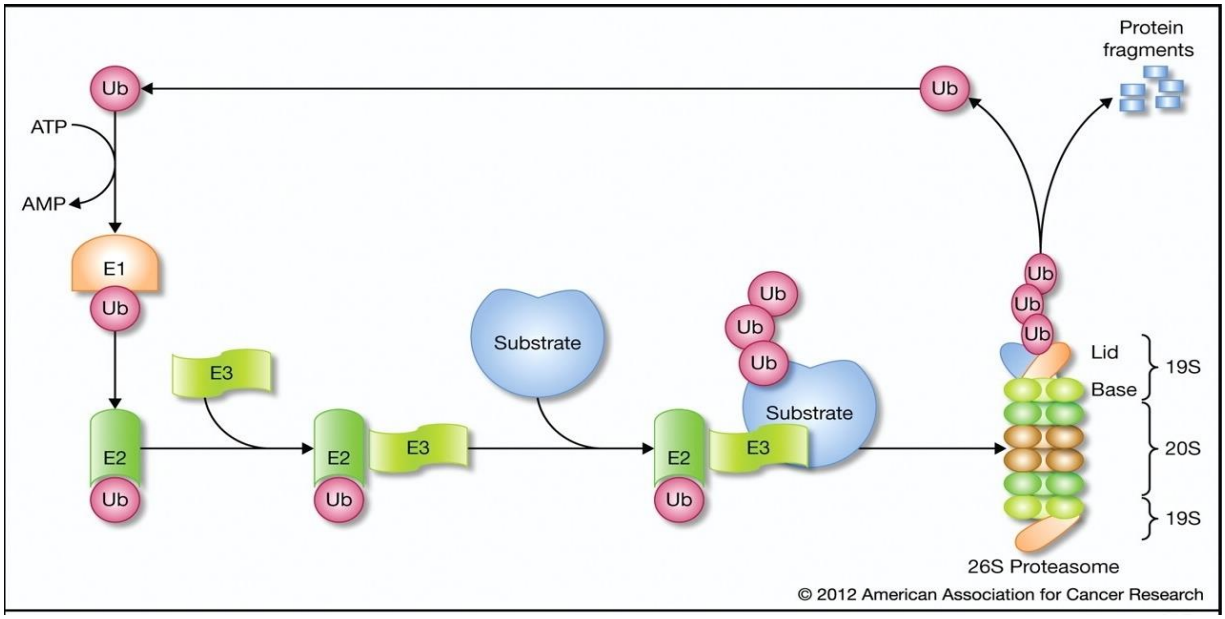

Image 5: Schematic image of UPS (from: American Association for Cancer Research 2012)

the increased conjugation of the ubiquitines or by the upregulation of transcripts belonging to the Ubiquitin-Proteasome machinery.

1.3.3 Ubiquitin Ligases (E3)

As it was mentioned before the role of these ligases is to conscript the ubiquitin enzymes (E2) where are attached ubiquitines, while at the same time

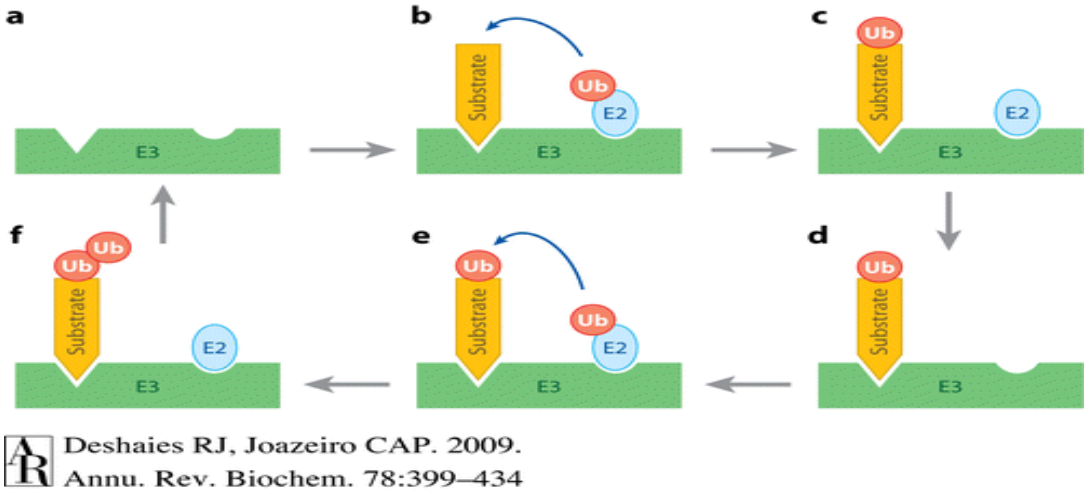

Image 6: Schematic image of ubiquitination of a protein. (The Ubiquitin Code in the Ubiquitin-Proteasome System and Autophagy, Yong Tae and Kwon'Correspondence, 2017)

adheres and recognizes a specific protein substrate. Then the ubiquitines through the aid of E3 are transferred to the protein. Ubiquitin is covalently attached to target proteins via an isopeptide bond between its C-terminal glycine and a lysine residue of the acceptor substrate. Now the protein is ubiquitinated. In this way the protein is targeted and can be degraded by the proteasome. The human genome encodes over 600 E3 ligases, although only a few have been characterized.

1.3.4 Classes of ubiquitin E3 ligases

There are three classes of ubiquitin E3 ligases. The HECT (homologous to E6-associated protein C-terminus), the RING and the U-box (a modified RING motif).

1.3.4.1 HECT domain E3s

In mammals, there are 30 HECT domain E3s. Among their many functions, HECT E3s have prominent roles in protein trafficking, the immune response, and in several signaling pathways that regulate cellular growth and proliferation [27]. The conserved HECT domain (which comprises ~350 amino acids) is located at the C-terminus of these enzymes, whereas their N-terminal domains are diverse and mediate substrate targeting. The HECT domain itself is bi-lobed, consisting of an N-terminal N-lobe that interacts with the E2 and a C-terminal C-lobe that contains the active-site cysteine that forms the thioester with ubiquitin [28]. The crystal structure of the NEDD4L HECT domain in complex with ubiquitin-conjugated E2 [UBCH5B~Ub, officially known as UBE2D2] shows the C-lobe contacting the esterified ubiquitin

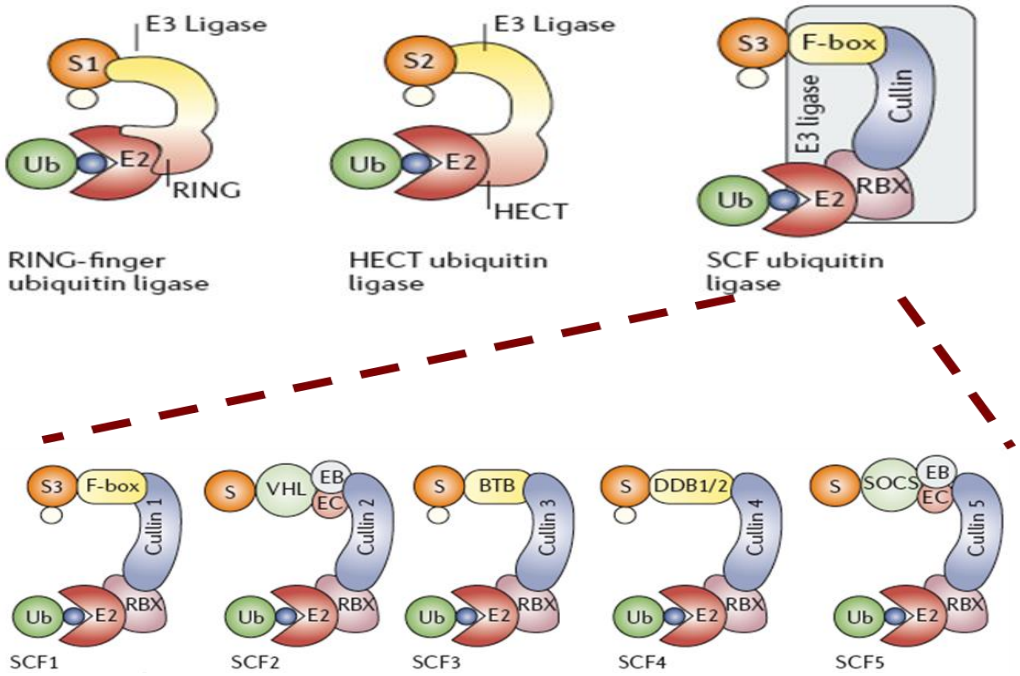

Image 7 : Schematic imaging of the ubiquitin E3 ligases (Modified form Nalepa & Harper , nrdd 2006)

and folding down onto UbcH5B, thereby making the distance between the E2 and E3 catalytic cysteines ~8Å [29]. By contrast, the first identified member of the HECT family, E6-associated protein (E6AP, officially known as UBE3A) [30], in complex

with its E2 UBCH7 (officially known as UBE2L3), shows the C-lobe in a more open architecture where the catalytic cysteine residues are 41Å apart [31]. Taken together, these and other structural studies [32],[33] suggest that the two lobes of the HECT domain are connected through a flexible hinge that allows them to come together during ubiquitin transfer. Interestingly, ubiquitin chain linkage specificity appears to be inherently dependent on the last 60 amino acids of the HECT domain C-lobe [34]).

1.3.4.2 RING finger E3s

The mammalian genome encodes more than 600 potential RING finger E3s [35]. A canonical RING finger is a Zn2+-coordinating domain that consists of a series of specifically spaced cysteine and histidine residues, and facilitates E2-dependent ubiquitylation [36]. The structure of the RING domain of Cbl in complex with an E2 illustrates several notable features of the RING domain [37]. The two zinc ions and the coordinating residues form a 'cross-brace' structure. Unlike the HECT domain, the RING finger domain does not form a catalytic intermediate with ubiquitin. Instead, the RING finger serves, at a minimum, as a scaffold that brings E2 and substrate together, and at least one study suggests that RING finger domains can also allosterically activate E2s [38].

Members of the RING finger ubiquitin ligase family can function as monomers, dimers or multi-subunit complexes. Dimerization generally occurs through the RING finger domain or surrounding regions and can result in homodimers [e.g. cIAP (cellular inhibitor of apoptosis, officially known as BIRC2), RNF4 (ring finger protein 4), SIAH (seven in absentia homologue 1), and TRAF2 (TNF receptor-associated factor 2) [39],[40],[41],[42] or heterodimers [e.g. MDM2 (murine double minute 2, also known as HDM2 in human) and MDMX (officially known as MDM4, also known as HDMX or HDM4 in human), BRCA1 (breast cancer 1) and BARD1 (BRCA1-associated RING domain 1), RING1b (officially known RNF2) and BMI1 (BMI1 polycomb ring finger oncogene)] [43],[44],[45],[46],[47],[48],[49]. For heterodimers, one RING domain (MDMX, BARD1, BMI1) often lacks ligase activity and might conform and/or stabilize the active E2-binding RING domain. Multi-subunit RING domains are exemplified by the cullin RING ligase (CRL) superfamily [50],[51], which includes the SCF complex, consisting of S-phase kinase-associated

protein 1 (SKP1), cullin and F-box protein, and the more elaborate anaphase-promoting complex/cyclosome (APC/C).

1.3.4.3 Cullin-RING ligases (CRLs)

Cullin-RING ligases (CRLs), the largest family of E3 ubiquitin ligases, account for ubiquitination of approximately 20 % cellular proteins degraded by UPS. The following part will describe briefly main features of CRLs, including their composition, and dynamic regulation of CRL assembly. Generally, CRLs consist of four elements: cullins, RING-finger proteins, adaptor proteins, and substrate recognition receptors.

The human genome encodes 8 cullins (CUL1, 2, 3, 4A, 4B, 5, 7, and 9, also known as PARC), 2 RING-finger proteins (RBX1 and RBX2, also known as ROC1 and ROC2/SAG, respectively), 4 adaptor proteins (SKP1 for CUL1/7, Elongin B/C for CUL2/5, and DDB1 for CUL4A/B), and more than 400 substrate recognition receptors (69 F-box proteins for CRL1, 80 SOCS proteins for CRL2/5, about 180 BTB proteins for CRL3, and 90 DCAF proteins for CRL4A/B). Thus, at least 400 CRLs can be assembled in human cells and regulate diverse biological processes by targeted ubiquitination and degradation of thousands of substrates.

1.3.4.4 Cul5-containing ubiquitin ligases

SOCS family

Suppressor of cytokine signaling (SOCS) proteins (SOCS1, SOCS2, SOCS3, SOCS4, SOCS5, SOCS6, and SOCS7) and cytokine-inducible Src homology 2 (SH2) domain-containing protein (CIS, also known as CISH) interact with Cul5 through its “Cul5 box”. The amino acid sequence LPΦP (Φ represents a hydrophobic residue) in the Cul5 box is required for specific interaction with Cul5. Cul5 also interacts with Rbx2, enabling SOCS box-containing proteins to form a protein complex with Cul5 and Rbx2. All SOCS family proteins have a

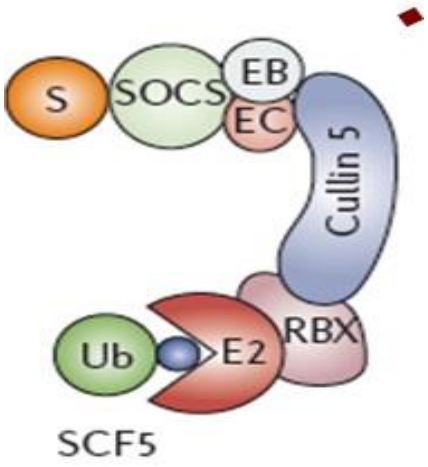

Image 8: Schematic imaging of the SCF. (Modified form Nalepa & Harper , nrdd 2006)

central SH2 domain and a C-terminally located SOCS box, which consists of an Elongin C-interacting BC box and a Cul5-interacting Cul5 box with an approximately 40-amino acid motif. By contrast, SOCS family proteins inhibit signaling by competing with downstream proteins for binding to the activated receptors, suppressing signal transduction by inducing the polyubiquitination and proteasomal degradation of target substrates.

1.3.4.5 Ankyrin repeat and SOCS box (ASB) family

The ASB family is composed of 18 members from ASB1 to ASB18. Several members interact with Cul5-Rbx2 and act as ubiquitin ligase complexes [52]. ASB-Cul5 complexes can oligomerize, and Cul5 can form heterodimeric complexes with the Cul4a-DDB1 complex [53].

Although ASB1 is expressed in multiple organs, including the hematopoietic compartment, ASB1-deficient mice develop normally and exhibit no phenotypes, except of diminished spermatogenesis and incomplete filling of seminiferous tubules [54].

ASB2 is induced by retinoic acid (RA) in acute promyelocytic leukemia cells, and exogenous ASB-2 in myeloid leukemia cells results in growth inhibition and chromatin condensation, which recapitulate the early steps of induced differentiation of acute promyelocytic leukemia cells [54]. ASB2 targets the actin-binding proteins filamin A and B for proteasomal degradation [55],[56],[57]. Knockdown of ASB2 in leukemia cells delays RA-induced differentiation, which suggests that ASB2 regulates hematopoietic cell differentiation by targeting filamins for degradation, thereby modulating actin remodeling [58]. ASB2 enhances the adhesion of hematopoietic cells to fibronectin, the main ligand of β1 integrins, by promoting filamin A degradation [59]. ASB2 heterodimerizes with Skp2 and forms a no canonical Cul1- and Cul5-containing dimeric ubiquitin ligase complex that promotes the polyubiquitination and degradation of Jak3 [60].A list of candidate substrates of ASB2 was reported in a recent study [60].

Tumor necrosis factor receptor type 2 (TNF-R2) is polyubiquitinated by ASB3 and targeted for proteasomal degradation [61]. Thereby, ASB3 negatively regulates TNF-R2-mediated cellular responses initiated by TNF-α [61].

Insulin receptor substrate 4 (IRS4) is expressed predominantly in the pituitary, thymus, and brain [62]. IRS4 is an adaptor molecule involved in signal transduction by both insulin and leptin, and is widely expressed throughout the hypothalamus [63]. ASB4 colocalizes and interacts with IRS4 in hypothalamic neurons and polyubiquitinates IRS4 for degradation to decrease insulin signaling [63]. Downregulation of ASB4 in HCC cells hinders cell migration and invasion, whereas overexpression of ASB4 increases the migration rate; ASB4 is downregulated by miR-200a [64] ASB4, which is highly differentially expressed in the vascular lineage during development [65], is an oxygen-sensitive ubiquitin ligase that is abundantly expressed in the developing placenta and is upregulated during the differentiation of embryonic stem cells into endothelial cell lineages [66].

Inhibitor of DNA binding 2 (ID2) negatively regulates vascular differentiation during development [67],[68]) and ASB4 promotes the ubiquitination and proteasomal degradation of ID2 [69]. ASB4-deficient mice phenocopy human pre-eclampsia, including hypertension and proteinuria in late-stage pregnant females, indicating that ASB4 mediates vascular differentiation in the placenta through the degradation of ID2 [69].

ASB6 is expressed in 3T3-L1 adipocytes but not in fibroblasts, and may regulate the insulin signaling pathway in adipocytes by promoting the degradation of adapter protein with a pleckstrin homology and SH2 domain (APS) [70].

The crystal structure of ASB9 with or without Elongin B and C has been determined [71],[72],[73]. ASB9 alone is unstable, whereas it forms a stable complex with Elongin B and C that also binds with high affinity to the Cul5N-terminal domain (Cul5NTD) but not to Cul2NTD [74]. ASB9 polyubiquitinates and decreases the levels of creatine kinase B (CKB) and ubiquitous mitochondrial creatine kinase (uMtCK) [75], [76], [77]. CK plays a major role in cellular energy metabolism in non-muscle cells [78]. CKB is overexpressed several of tumors, including neuroblastoma, small cell lung carcinoma, colon and rectal adenocarcinoma, and breast and prostate carcinoma [78], [79]. Furthermore, high ASB9 mRNA expression is correlated with good prognosis, and knockdown of ASB9 increases colorectal cancer (CRC) cell invasiveness [80]. ASB9 upregulation may result in a good prognosis for CRC by promoting the degradation of CKB and uMtCK.

The Notch signaling pathway is essential for the spatio-temporal regulation of cell fate [81], [82]. The single-pass transmembrane protein delta acts as a ligand for the Notch receptor. Danio rerio Asb11 (d-Asb11) regulates compartment size in the endodermal and neuronal lineages by promoting the ubiquitination and degradation of deltaA but not deltaD, leading to the activation of the canonical Notch pathway [83], [84]. Knockdown of d-Asb11 downregulates specific delta-Notch elements and their transcriptional targets, whereas these are induced when d-Asb11 is misexpressed in zebrafish embryos [83]. These data indicate that d-Asb11 regulates delta- Notch signaling for the fine-tuning of lateral inhibition gradients between deltaA and Notch [83]. Mutant zebrafish lacking the Cul5 box, which results in the inability to degrade delta, are defective in Notch signaling, as indicated by the impaired expression of Notch target genes [85].

Forced expression of d-asb11 impairs terminal differentiation and increases proliferation in the myogenic progenitor compartment [86]. By contrast, mutation of d-asb11 causes premature differentiation of muscle progenitors and delays regenerative responses in adult injured muscle, suggesting that d-asb11 is a principal regulator of embryonic as well as adult regenerative myogenesis [86]. ASB11 is an endoplasmic reticulum (ER)-associated ubiquitin ligase that promotes the ubiquitination and degradation of Ribophorin 1, an integral protein of the oligosaccharyltransferase (OST) glycosylation complex, which N-glycosylates newly synthesized proteins in the rough ER.

1.4. Asb2 isoforms

Ankyrin repeat and SOCS box containing 2 beta (Asb2β), one on the two transcript variants of the ASB2 gene, is a novel muscle-specific E3 ubiquitin ligase that regulates muscle differentiation [87]. Two ASB2 isoforms have been described: ASB2 a and ASB2 b that are involved in hematopoietic [88] and myogenic [87] differentiation, respectively.

Among the hundreds of E3 ubiquitin ligases, only few have been found to regulate muscle mass. Knockdown of either one of these genes partially protects from muscle atrophy [89], [90], [91], [92]. ASB2beta is expressed in muscle cells during

embryogenesis and in adult tissues. Indeed, ASB2beta is the specific subunit of an E3 ubiquitin ligase that exerts its functions through the degradation of its substrates by the proteasome.

ASB2beta is part of an active E3 ubiquitin ligase complex and targets the actin-binding protein filamin B (FLNb) for proteasomal degradation. Thus, ASB2beta regulates FLNb functions by controlling its degradation. Knockdown of endogenous ASB2beta by shRNAs during induced differentiation of C2C12 cells delayed FLNb degradation as well as myoblast fusion and expression of muscle contractile proteins. Finally, knockdown of FLNb in ASB2beta knockdown cells restores myogenic differentiation. Altogether, is suggested that ASB2beta is involved in muscle differentiation through the targeting of FLNb to the proteasome. [87]

Filamins (FLNs) make up one important class of actin-binding and cross-linking proteins. Vertebrate FLNs are non-covalent dimers of 240–280 kDa subunits composed of an N-terminal actin-binding domain followed by 24 tandem immunoglobulin-like domains (IgFLN1–24), the last of which mediates dimerization [93], [94]. Hinges between IgFLN15 & 16 (H1) and IgFLN23 & 24 (H2) result in a V-shaped flexible actin-crosslinker capable of stabilizing orthogonal networks with high-angle F-actin branching [95]. In addition, FLNs bind many transmembrane receptors, signaling and adapter proteins [94], [96], [97]. Through these interactions, often mediated by IgFLN16–24, FLNs complex multiple partners near one another, potentially enhancing signal transduction by aiding assembly of networks linking receptors with signaling proteins and the cytoskeleton [94].

Interestingly, only the overexpression in muscles of Asb2b, and not of the other E3 ligases, such as Atrogin1, MuRF1 or MUSA1, is sufficient to induce muscle atrophy [98], [99], [100]. However, how, mechanistically Asb2b activates an atrophy program and which are its specific substrates are unexplored issues. According to the literature, Asb2b is a novel regulator of muscle mass because Asb2b is a TGF-b network-responsive negative regulator of muscle mass [98] and reduced levels of Asb2b are associated with hypertrophic cardiomyopathy [101].

In addition, Asb2b is a circadian gene, which might control rate-limiting steps in metabolic pathways to prepare the organism for daily environmental changes [102].

Interestingly, chronic disruption of circadian clocks components has consistently been linked to metabolic disorders and diseases [103] .

In this project, we will use muscle-specific Asb2β knockout mice to unravel the link between muscle mitochondrial/metabolic control and muscle mass regulation.

Aim

The Ubiquitin Proteasome System (UPS) is one of the major mechanisms that control proteolysis and ubiquitination of protein substrates. The specificity of ubiquitin-dependent degradation derives from many E3s that recognize specific substrates. This work is based on the study of the role of Asb2β in vivo, a new E3 muscle-specific ubiquitin ligase. To understand its role, we have generated skeletal muscle specific knock-out mouse models and we analyzed its function in physiological and in muscle wasting conditions.

According to the literature, Asb2β is a novel regulator of muscle mass because Asb2b is a TGF-b network-responsive negative regulator of muscle mass [98] and reduced levels of Asb2β are associated with hypertrophic cardiomyopathy [101]. In addition, Asb2β is a circadian gene, which might control rate-limiting steps in metabolic pathways to prepare the organism for daily environmental changes [102] Interestingly, chronic disruption of circadian clocks components has consistently been linked to metabolic disorders and diseases. Taken together, Asb2β is a very attractive candidate to investigate the role of mitochondrial dysfunction and metabolic changes in skeletal muscle mass regulation. In this project, we will use muscle-specific Asb2β knockout mice to unravel the link between muscle metabolic control and muscle mass regulation.

The main goal of the present project is to investigate *in vivo* the role of Asb2β in muscle metabolism and function using mice models. From our preliminary results, (in younger mice 3-5), interestingly, Asb2b defective muscles showed normal muscle architecture but we observed an accumulation of glycogen store, suggesting that the lack of Asb2b could be important to maintain skeletal muscle homeostasis. The aim of this project is to characterize the role of Asb2b in long-term deletion (18 months) mouse models. It is hypothesized that Asb2β leads to enhanced pathological phenotype. Using this long-term knockout model, we will investigate the relevance of prolonged Asb2β ablation. With this work we suggest a muscle atrophy scenario, in order to increase the specificity of therapeutic interventions of the future.

2. EXPERIMENTAL PART

This work is based on the study of the role of Asb2β, a new E3 muscle-specific ubiquitin ligase. To understand its role, we have generated skeletal muscle specific knock-out mouse models and we analyzed its function in physiological and in muscle wasting conditions.

The prediction is that Asb2β deletion leads to significant changes in the catabolic pathways controlling muscle mass. We expect to elucidate in vivo pathways important for muscle mass regulation and function that are controlled by Asb2β.

Firstly, we performed histological analysis on the KO mice and compered them to the mice that we used as controls (Asb2β f/f). To have a full image of the fiber structure we also performed staining (H/E for the fiber and SDH for the mitochondrial structure).

We, also, hypothesize that Asb2β controls muscle function and metabolism. Since other muscle-specific E3s, such as Atrogin1 and MuRF1, are central for the turnover of glucose metabolic key enzymes, we wondered whether Asb2β has a role in carbohydrate metabolism. So we applicate the PAS staining and to confirm the image result, we also performed assays to measure the glycogen storage. Furthermore, we performed in vivo experiments to revel if there is any alteration of the glycogen homeostasis such as GTT, PTT and ITT.

Another expectation is to find alterations in the mitochondrial network and function leading to reduced energy production in KO muscles. For that reason we will examinate the mitochondrial structure by staining. Moreover, to examine the mitochondrial function, we measured fusion and fission specific proteins by using Western blots. To measure the oxidative stress we performed Oxyblot.

Finishing, executing exhaustion experiments we wanted to observe if there is any difference on the physical dynamic of the muscles of the KO mice.

This research project was conducted in the VIMM institute, and the lab was directed by Marco Sandri. The project was running under the supervision of Vanina Romanello. The present thesis was under the scientific diligence by Dr. Androniki Papoutsi, Associate Professor of Biology and Genetics, Department of Medical Laboratory Studies, in Alexander Technological Educational Institute of Thessaloniki.

2.1. MATERIALS AND METHODS

2.1.1 Animal handling and generation of muscle-specific Asb2b knockout mice.

Animals were handled by specialized personnel under the control of inspectors of the Veterinary Service of the Local Sanitary Service (ASL 16 - Padova), the local officers of the Ministry of Health. All procedures are specified in the projects approved by the Italian Ministero Salute, Ufficio VI (authorization numbers 1060/2015 PR). Muscles were removed at various time periods and frozen in liquid nitrogen for subsequent analyses.

To avoid any compensation or adaptation, which can occur when the gene is deleted during embryonic development, we use the tamoxifen-inducible technology by crossing the Asb2β f/f line with mice carrying Cre-ER driven by human skeletal actin promoter (HSA) to generate the iAsb2β-/- transgenic mice (hereafter referred as KO) or the control iAsb2β f/f mice (hereafter referred as WT).We set-up a tamoxifen treatment protocol to efficiently reduced Asb2β transcripts. PCR genotyping was performed with the following primers:

Ef: CAGTGTCTGCTCTGAGGTCTCTC

Lf: CTAGATAGCTCTACAGCTAATTCCG

Er: CAATCTCTCCCTGGTAGAAACAGTTTGG

Cre Fw: CACCAGCCAGCTATCAACTCG

Cre Rv: TTACATTGGTCCAGCCACCAG

Also, there is a second line used. We crossed Asb2β f/f with transgenic mice expressing Cre-recombinase under the control of a Myosin Light Chain 1 fast promoter (MLC1f-Cre) [104] to generate mAsb2β-/- transgenic mice (hereafter referred as KO or ASB2β-/-) or corresponding control mAsb2βf/f mice (hereafter referred as WT). This approach takes advantage of the muscle specific and early expression of MLC1f promoter, which starts to be active during development at 13 days post coitum. Therefore, Asb2β deletion may occur during late embryo development or early postnatal life only in skeletal muscle tissue. PCR analysis

confirmed the deletion of the floxed sequence in genomic DNA extracted from skeletal muscle.

2.1.2 Histology analyses and fiber size measurements

Muscles were collected and directly frozen by immersion in liquid nitrogen. Then we cut muscle 10µm thick cryosections by using Cryostat (Leica CM 1950). TA cryosections, were used to analyze tissue morphology with different methods, reported below. Images were collected with an epifluorescence Leica DM5000B microscope, equipped with a Leica DFC300-FX digital charge-coupled device camera, by using Leica DC Viewer software.

2.2.1 Haematoxilin and Eosin staining (H&E)

Haematoxilin colors basophilic structures that are usually the ones containing nucleic acids, such as ribosomes, chromatin-rich cell nuclei, and the cytoplasmic regions rich in RNA. Eosin colors eosinophilic structures bright pink. The eosinophilic structures are generally intracellular or extracellular protein. The methods consist of:

Materials	Time
PFA 4%	10 minute
3 washes in PBS	5 minutes each
Harris Hematoxylin (SIGMA)	6 minute
Wash in running tap water	3 minutes
Alcoholic acid	10 seconds
Wash in running tap water	3 minutes
Eosin Y Solution Alcoholic (SIGMA)	1 minute
Dehydratation	
Ethanol 70%	5 minutes
Ethanol 95%	2 minutes
Ethanol 100%	3 minutes
Xilen 1	5 minutes
Xilen 2	5 minutes
Mount with Eukitt (Sigma-Aldrich)	

2.3 Succinate dehydrogenase (SDH)

The succinate dehydrogenase is an enzyme complex, bound to the inner mitochondrial membrane. With this staining it is possible to evaluate approximately the quantity of mitochondria present in the muscle fibers, through colorimetric evaluation. The reaction gives a purple coloration in the oxidative fibers. The sections were incubated for 30 minutes at 37°C with SDH solution (0.2M sodium succinate) (Sigma Aldrich),0.2M phosphate buffer (Sigma) ph. 7.4 and 50mg of nitro blue tetrazolium (NBT) (Sigma Aldrich).After the incubation, the sections were washed 3 minutes with PBS and then mounted with Mounting medium (Dako)**.**

2.4 Periodic acid Schiff (PAS)

This method is used to identify glycogen in tissues.The reaction of periodic acid selectively oxidizes the glucose residues, creates aldehydes that react with the Schiff reagent and creates a purple-magenta color. A suitable basic stain is often uded as a counter stain. The sections were treated with:

Materials	Times
Fix in Carnoy's fixative	5 minutes
Wash in water	3 times
0.5% periodic acid	5minutes
Wash in water	3 times
Schiff's solution (Sigma)	10 minutes
Wash in running tab water	10 minutes
Mount with Elvanol	

2.5 Fiber cross-sectional area (CSA)

Fiber Cross-Sectional Area was measured, by using SMASH [105]. All data are expressed as the mean SEM (error bars). Comparisons were made by using t test, with $p<0.05$ being considered statistically significant.

2.6 Immunoblotting

Cryosections of 20µm of TA muscles were lysed with 100µl of a buffer containing 50mM Tris pH 7.5, 150mM NaCl, 10mM MgCl2, 0.5mM DTT, 1mM EDTA, 10% glycerol, 2% SDS, 1% Triton X-100, Roche Complete Protease Inhibitor Cocktail and Sigma Protease Inhibitor Cocktail. After incubation at 70°C for 10 minutes and centrifugation at 11000 g for 10 minutes at 4°C, the surnatant protein concentration was measured using BCA protein assay kit (Pierce) following the manufacturer's instructions.

2.7 Protein gel electrophoresis

The extracted proteins from TA muscle were solubilized in Loading buffer composed by 5µl of 4X NuPAGE® LDS Sample Buffer (Life Technologies) and 1µl of 20X DTT (Life Technologies). The volume of each sample was brought to 20µl with SDS 1X. The samples were denatured at 70°C for 10 minutes. Samples were loaded on SDS 4-12% precast polyacrylamide gels (NuPAGE Novex-Bis-trisgels) or in SDS 3-8% depending on the protein to be analyzed (Life Technologies). The electrophoresis was run in 1X MES/MOPS Running buffer or 1X Tris-Acetate Running buffer respectively (Life Technologies) for 1 hour and 30 minutes at 150V constant.

2.8 Protein Oxidation Detection

EDL muscles were lysed with 100µl of a buffer containing 50mM Tris pH 7.5, 150mM NaCl, 10mM MgCl2, 0.5mM DTT, 1mM EDTA, 10% glycerol, 2% SDS, 1% Triton X-100 and Roche Complete Protease Inhibitor. Add a metallic bit to each sample. Insert the samples into the TissueLyser II (simultaneously disrupts samples through high-speed shaking) set it at 30fr. for 1 min. Centrifuge at 11000 g for 10 minutes at 4°C, the surnatant protein concentration was measured using Bradford protein assay kit following the manufacturer's instructions.

The extracted proteins were solubilized in 1µl of 20X DTT (Life Technologies) and 5µl SDS 1X. The volume of each sample was brought to 20µl with loading buffer composed of 4X NuPAGE® LDS Sample Buffer (Life Technologies). The samples were denatured at room temperature for 10 minutes. For the reaction it was used 5µl (+/- 10µg) of the sample to analyze. To solubilize, 5µl of 12% SDS and for the derivatization 10µl of mM DNPH in 10% TFA. Incubate at room temperature for 20 min to end the reaction 10µl of 2M Tris base pH 7.5 in 30% glycerol. Samples were loaded on SDS 12% precast polyacrylamide gels (NuPAGE Novex-Bis-trisgels). The electrophoresis was run in 1X MES/MOPS Running buffer or 1X Tris-Acetate Running buffer respectively (Life Technologies) for 1 hour and 30 minutes at 150V constant.

The final result of the OxyBlot procedure will show several bands in the derivatization reaction sample of each condition. Bands that are present in the derivatization reaction but not in the negative control have undergone oxidative modifications. The degree of protein oxidation can be identified by the intensity of the bands. That is, the more intense the bands are, the higher is the degree of stress specific protein oxidation.

2.9 Transfer of the protein to the nitrocellulose membrane

After the electrophoretic run, proteins were transferred from gels to nitrocellulose membranes. The gel and the membrane were equilibrated in Transfer Buffer. The Transfer Buffer was prepared as follows: 50ml of 20X NuPAGE® Transfer buffer (Life Technologies), 1ml of 10X NuPAGE® Antioxidant (Life Technologies), 200ml of 20% Methanol (Sigma-Aldrich). The volume was brought to 1L with distilled water. The blotting was obtained by applying a current of 400mA for two hours at 4°C. To evaluate the efficiency of the transfer, proteins were stained with Red Ponceau 1X (Sigma-Aldrich). The staining was easily reversed by washing with distilled water.

2.10 Incubation of the membrane with antibodies

Once the proteins were transferred on membranes, the membranes were saturated with Blocking Buffer (5% no fat milk powder or BSA solubilized in TBS

1X with 0.1% TWEEN) for 1 hour at room temperature and were incubated overnight with various primary antibodies at 4°C. Membranes were then washed 3 times with TBS 1X with 0.1% TWEEN at room temperature (RT) and incubated with secondary antibody-HRP Conjugate (Bio-Rad), for 1 hour at RT. Immunoreaction was revealed by substrates for detection of horseradish peroxidase (HRP) enzyme activity via Pierce ECL Western Blotting Substrate via chemilumescent (ECL). To deduct the signal we used ImageQuant LAS 4000, which performs digital imaging with a CCD camera-based imager or a scanner, depending on the characteristics of the light emitted from the detectionsystem.

Blots were stripped using Stripping Solution, containing 25mM glycine and 1% SDS, pH 2.

Antibody	Costumer	Dilution	Analysis
Rabbit anti-LC3	Sigma L7543	1:1000	WB
Rabbit anti-Bnip3	Cell Signaling #3769	1:1000	WB
Mouse anti-Drp1	BD 611738	1:2000	WB
Mouse anti-GAPDH	Abcam ab8245	1:10000	WB
Mouse anti-Porin	Santa cruz Sc-11415	1:10000	WB
Rabbit anti-TOM20	Abcam ab14734	1:10000	WB
Rabbit anti FoxO1	Cell signaling	1:1000	WB
Rabbit anti-actin	Abcam A4700	1:1000	WB

2.11 Glycogen Assay

Glycogen is a branched polymer of glucose that serves as the primary short-term energy storage molecule in animals. Glycogen is primarily synthesized in liver and muscle tissue where it can constitute up to 10% of the weight of liver and 1-2% of the weight of muscle tissue. While muscle glycogen is generally utilized locally, liver glycogen serves as an important buffer to regulate blood glucose levels.Glycogen concentration is determined by a coupled enzyme assay, which produces a colorimetric (570 nm) product, proportional to the glycogen present.

For this experiment we used the Carbohydrate Metabolism Assay Kit from Sigma (MAK016 SIGMA).

Components

Hydrolysis Buffer
Development Buffer
Fluorescent Peroxidase Substrate in DMSO
Hydrolysis Enzyme Mix
Development Enzyme Mix
Glycogen Standard, 2 mg/mL

Standards preparation:

10 mL of the 2.0 mg/mL Glycogen Standard were diluted with 90 mL of ultrapure water to prepare a 0.2 mg/mL standard solution. 0, 2, 4, 6, 8, and 10 mL of the 0.2 mg/mL standard solution were added into a 96 well plate, generating 0 (assay blank), 0.4, 0.8, 1.2, 1.6, and 2.0 mg/well standards. Hydrolysis Buffer was added to each well to bring the volume to 50 mL. In the final results we should have a standard curve that will help us calculate the concentration of the glycogen in the samples.

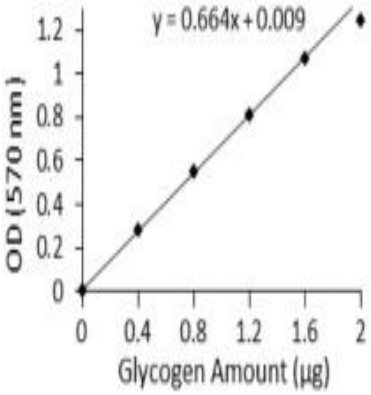

Image 9: Standard curve (Glycogen Assay)

Sample preparation:

Tissue (±10 mg) was homogenized in 100 mL of water on ice. The homogenates were boiled for 5 minutes to inactivate enzymes and then centrifuged at 13,000 ´ g for 5 minutes to remove insoluble material. Lastly the samples were drought to a final volume of 50 mL with Hydrolysis Buffer.

Reaction:

2 mL of the Hydrolysis Enzyme Mix were added to colorimetric assays, and were incubated for 30 minutes at room temperature. 50 mL of the Master Reaction Mix were required for each reaction (well). 50 mL of the Master Reaction Mix were added to each of the wells and the reaction was incubated for 30 minutes at room temperature. We measured the absorbance at 570 nm (A570).Concentration of Glycogen:

Sa/Sv = C

(Sa= Amount of glycogen in unknown sample (mg) from standard curve

Sv = Sample volume (mL) added into the wells

C = Concentration of glycogen in sample)

2.12.1 Gene expression analysis

2. 12.2 Extraction of RNA

Total RNA was isolated from gastrocnemius muscle using Trizol (Life Technologies) following the manufacturer's instructions.

2.12.3 Synthesis of the first strand of cDNA

400ng of total RNA was reversely transcribed with SuperScriptTM III (Life Technologies) in the following reaction mix:

Random primer hexamers (50ng/µl random): 1µl dNTPs 10mM: 1µl The volume was adjusted to 13µl with RNase-free water.

The samples were mixed and briefly centrifuged and denatured by incubation for 5 minutes at 65°C to prevent secondary structures of RNA. Samples were incubated on ice and the following components were added sequentially:

First strand buffer 5X (Life Technologies): 4µl DTT 100mM: 1µl Rnase Out (Life Technologes): 1µl SuperScriptTM III (Life Technologies): 1µl H2O RNase-free: 0.5µl

The used reaction program was:

step1: 25°C for 10 minutes step2: 42°C for 50 minutes step3: 70°C for 15 minutes

At the end of the reaction, the volume of each sample was adjusted to 30µl with RNase free water.

2.12.4 Real-Time PCR reaction

Quantitative real-time PCR was performed with SYBR Green chemistry (Applied Biosystems). SYBR green is a fluorescent dye that intercalates into double-stranded DNA and produces a fluorescent signal. The real-time PCR instrument allows real time detection of PCR products as they accumulate during PCR cycles and create an amplification plot, which is the plot of fluorescence signal versus cycle

number. In the initial cycles of PCR, there is little change in fluorescence signal. This defines the baseline for the amplification plot. An increase in fluorescence above the baseline indicates the detection of accumulated PCR products. A fixed fluorescence threshold can be set above the baseline. The parameter Ct (threshold cycle) is defined as the fractional cycle number at which the fluorescence passes the fixed threshold. So the higher the initial amount of the sample, the sooner the accumulated product is detected in the PCR process as a significant increase in fluorescence, and the lower is the Ct value.

1µl of diluted cDNAs was amplified in 10µl PCR reactions in an ABI Prism 7000 (Applied Biosystem) thermocycler, coupled with an ABI Prism 7000 Sequence Detection System (Applied Biosystems) in 96-wells plates (Micro Amp Optical, Applied Biosystems). In each well 5µl sample mix and 5µl reaction mix were mixed. Sample mix was prepared as follows for 5µl total volume:

Template cDNA: 1 µl H2O Rnase-free: 4 µl

The SYBR Green qPCR (Applied Biosystem) was used for the real-time PCR reaction as follows:

SYBR Green qPCR (Applied Biosystem): 4.8µl Mix Primer forward /reverse 50mM: 0.2µl

The PCR cycle used for the Real-Time PCR was:

step1: 95° C for 15 minutes

step2: 95° C for 25 seconds

step3: 58° C for 1 minute

step4: go to step 2 for 40 times

2.12.5 Quantification of the PCR products and determination of level of expression

A relative quantification method were used to evaluate the differences in gene expression, as described by Pfaffl [106]. In this method, the expression of a gene is determined by the ratio between a test sample and a housekeeping gene. The relative expression ratio of a target gene is calculated based on the PCR efficiency (E) and the threshold cycle deviation (ΔCt) of unknown samples versus a control, and expressed in comparison to a reference gene. The mathematical model used for relative expression is represented in this equation:

$$R = \frac{(E_{target})^{\Delta CPtarget\,(control - sample)}}{(E_{ref})^{\Delta CPref\,(control - sample)}}$$

The internal gene reference used in our real time PCR was gapdh, whose abundance did not change under the experimental conditions.

2.13 STATISTICAL ANALYSIS AND EXPERIMENTAL DESIGN

The sample size was calculated using size power analysis methods for a priori determination based on the s.d., and the effect size was previously obtained using the experimental methods employed in the study. For animal studies, we estimated sample size from expected number of knockout mice and littermate controls, which was based on mendelian ratios. We calculated the minimal sample size for each group by at least four organisms. Considering a likelydrop off effect of 10%, we set sample size of each group at five mice. To reduce the s.d., we minimized physiological variation by using homogenous animals with same sex and same age. The exclusion criteria for animals were pre-established. In case of death, cannibalism or sickness, the animal was excluded from analysis. Tissue samples were excluded in cases such as cryoartefacts, histological artifacts or failed RNA extraction. We included animals from different breeding cages by random allocation to the different experimental groups. Animal experiments were not blinded, however, when applicable, the experimenters were blinded to the nature of samples by using number codes until final data analysis was performed.

Statistical tests were used as described in the figure legends and were applied on verification of the test assumptions (for example, normality). Generally, data were

analyzed by two-tailed Student's t-test. For all graphs, data are represented as means±s.e.m. For the measurements variables used to compare KO animals versus controls, or innervated animals versus denervated ones, the variance was similar between the groups.

2.13. Treadmill test: latency to exhaustion

1. Mice are familiarized with the treadmill two days prior to the experiment by exercising them for 10 minutes at 18m/min.

2. On the day of the experiment, the mouse is placed in the stopped treadmill for 5 min to acclimatize

3. The treadmill is equipped with a shock pad. Shocks are set at 0.2mA, 200ms pulses, 4Hz.

4. Treadmill is started at 18m/min.

5. After 3 min, speed is increased by 4m/min.

6. Every three minutes thereafter, speed is increased by 4m/min until mouse has reached exhaustion

Image 10: Treadmill test in vivo.

Exhaustion is defined as the point at which the mouse remains on the shock pad for 5 continuous seconds.

7. Once exhaustion is reached, the mouse is moved to the cage to recover.

Speed	Minutes of running
17 cm/sec	For 40’
18 cm/sec	For 10’
20 cm/sec	For 10’
22 cm/sec	For 10’
23 cm/sec	For 5’
25 cm/sec	For 5’

We increase the distance every 5 minutes until the animal reaches exhaustion.

The electrical voltage is always 0,2.

2.14 Glucose tolerance test (GTT)

Glucose tolerance test is a standard procedure that addresses how quickly exogenous glucose can be cleared from blood. Specifically, uptake of glucose from the blood by cells is regulated by insulin. Impairment of glucose tolerance (i.e, longer time to clear given amount of glucose) indicates problems with maintenance of glucose homeostasis (insulin resistance, carbohydrate metabolism, diabetes, etc).

Reagents and Equipment:

1. 70% ethanol
2. Beta-D(+)-glucose (Sigma-Aldrich, catalog number: G8270)
3. NaCl
4. KCl
5. Sodium phosphate
6. Phosphate buffered saline (PBS)
7. BD logistic glucometer
8. BD glucose test strips
9. 27 gauge needle (Single-Use Needles)
10. Microvette CB300 Z serum
11. Clean mouse cages

Procedure

- Fast animals in fresh cages with water supply for ~8 h the day of the experiment.
- Monitor body weight as well as baseline blood glucose level for each animal.
- Prepare 10% glucose in 1x PBS and sterilize the solution by 0.2 μm-filtration.
- Prepare injection solution in a 0.5 ml eppendorf tube for each animal (2 mg glucose/g body weight). Volume (μl) = Body Weight (g) x 20. Use 20% glucose instead, should the body weight be greater than 30 g.
- Sterilize abdominal region of animal with 70% ethanol, and clean up with dry cotton ball. Hold the back of the animal firmly, and inject glucose intraperitoneally into recipient subject with a 27-gauge sterile needle.

- Perform injection slowly with an angle of 30 to 45 °C to avoid subcutaneous injection. Pick the injection site away from the liver and close to the ventral axis to avoid kidney damage.
- Put the animal back into the cage and measure blood glucose levels at 15, 30, 60, 90 and 120 min (or 30, 60, 90, 120 and 240 min). At least 3-4 replicate animals should be used for each time-point.
- Upon completion, provide food to each mouse and return the mice to the mouse colony.

2.15 Insulin tolerance test (ITT)

Reagents and equipment:

1. insulin syringe
2. human insulin 100 IU
3. 0.9 % sterile saline
4. BD logistic glucometer
5. BD glucose test strips
6. Clean mouse cages
7. 70% EtOH
8. 27 gauge needle (Single-Use Needles)

Procedure:

- Fast animals in fresh cages with water supply for ~8 h the day of the experiment.
- Monitor body weight as well as baseline blood glucose level for each animal.
- Calculate the insulin dose for each mouse (based on body weight).
- Prepare 0.25 IU insulin solution by diluting insulin in sterile saline (and sterile tubes) in 1:400 concentration
- Dispense the required volume of insulin solution for each mouse into separate 1.5 ml tubes (Volume is calculated as follows: 0.75 IU insulin/g BW). Vol (µl) = 3 x BW

- Measure blood glucose of the 1st mouse from tail blood by using a needle opening a hole on the tail tip.
- Perform intraperitoneal injection (i.p.) of insulin. Record blood glucose level(s).
- Repeat blood glucose measurement at 15', 30', 45', 60', and 90' by reopening the tail wound each time.
- Upon completion, provide food to each mouse and return the mice to the mouse colony.

2.16 Pyruvate tolerance test (PTT)

Glucose homeostasis is tightly controlled by the interplay of various hormones and organs. In the fasted state, glucose levels are prevented from dropping too low (hypoglycemia) through two hepatic processes: glycogenolysis, the degradation of glycogen and gluconeogenesis, the generation of glucose from non-carbohydrate carbon substrates including pyruvate and lactate (produced by anaerobic metabolism of glucose in muscles). Injection of pyruvate bolus elicits a glycemic excursion that reflects hepatic gluconeogenesis.

Reagents and equipment:

1. 2.5g pyruvate in 10 mL PBS- This will correspond to 2.5 g/kg injections.
2. BD logistic glucometer
3. BD glucose test strips
4. 27 gauge needle (Single-Use Needles)
5. Clean mouse cages
6. 70% EtOH

Procedure:

- Fast animals in fresh cages with water supply for ~8 h the day of the experiment.
- Monitor body weight as well as baseline blood glucose level for each animal.
- Prepare pyruvate syringes with 10 uL per g mouse weight (ie for a 30g mouse, 300 uL).
- Inject appropriate amount of pyruvate into interperitoneal cavity of the mouse.

- Immobilize mouse and restrain tail with one hand
- Aim needle between the midline and the hip bone
- Insert syringe (do not inject) into cavity
- Eject syringe.
- Repeat blood glucose measurement at 15', 30', 45', 60', and 90' by reopening the tail wound each time.
- Upon completion, provide food to each mouse and return the mice to the mouse colony.

3. RESULTS

3.1. Generation of muscle -specific Asb2β knockout mice

We crossed Asb2βf/f with transgenic mice expressing Cre- recombinase under the control of a Myosin Light Chain 1 fast promoter (MLC1f-Cre) [104], to generate mAsb2β-/- transgenic mice (hereafter referred as KO) or corresponding control mAsb2βf/f mice (hereafter referred as WT). This approach takes advantage of the muscle specific and early expression of MLC1f promoter, which starts to be active during development at 13 days post coitum. Therefore, Asb2β deletion may occur during late embryo development or early postnatal life only in skeletal muscle tissue. PCR analysis confirmed the deletion of the floxed sequence in genomic DNA extracted from skeletal muscle (Fig. 11A). Deletion of the Asb2β gene was further confirmed by Asb2β mRNA levels in Tibialis anterior muscles (Fig.11B). The resulting mAsb2β-/- knockout animals are fully viable, fertile and indistinguishable in appearance from control Asb2βf/f (image 11).

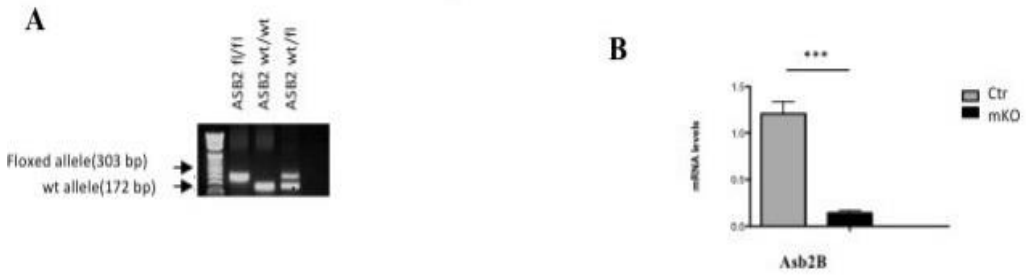

Image 11: A) Genotyping of KO mice. An efficient CRE-mediated combination of lox P sites (-/-) was determinate by PCR analysis of muscle genome DNA. B) Quantitative RT-PCR shows that mRNA levels of Asb2β are downregulated in muscles of muscle-specific Asb2β KO mice. Data present mean + s.e.m (***, p< 0,0001) .

Another generation that was used for the experiments. To generate inducible muscle-specific deletion of Asb2 was obtained by crossing the Asb2bf/f line with mice carrying Cre-ER driven by human skeletal actin promoter (HSA). Tamoxifen-induced Cre LoxP recombination was activated by oral administration of tamoxifen-containing chow (Tam400/Cre ER Harlan) which was administrated ad libitum for 3

weeks. Muscles were collected 3 months after the tamoxifen diet finished. Cre-negative littermates, also receiving tamoxifen treatment, were used as controls. Adult mice (18 and 15 months-old) of the same sex and age were used for each individual experiment.

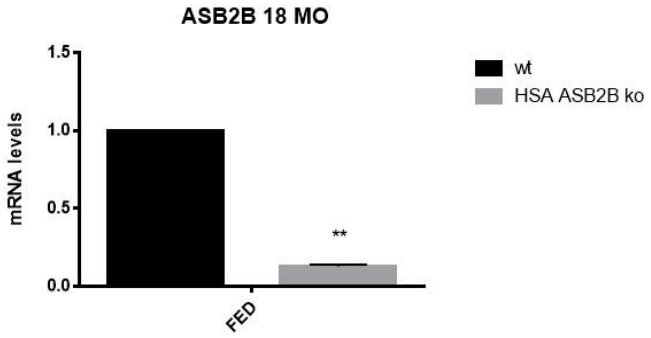

Image 12: Quantitative RT-PCR shows that mRNA levels of Asb2β are downregulated in muscles of muscle-specific Asb2β KO mice. Data present mean + s.e.m (**, p< 0,001)

3.2. Asb2β deletion in muscle impacts muscle homeostasis.

To address the relevance of long-term Asb2β ablation, we analysed muscles from 18 months-old control and knockout mice in fed and starved conditions.

The resulting Asb2β--/-- mice were indistinguishable in appearance from age-matched control Asb2βf/f mice. Histological analysis of adult muscles revealed a different muscle architecture and presence.

More specific with H/E staining we had a more “lose” structure between the muscle fibers in the Asb2β--/-- mice.

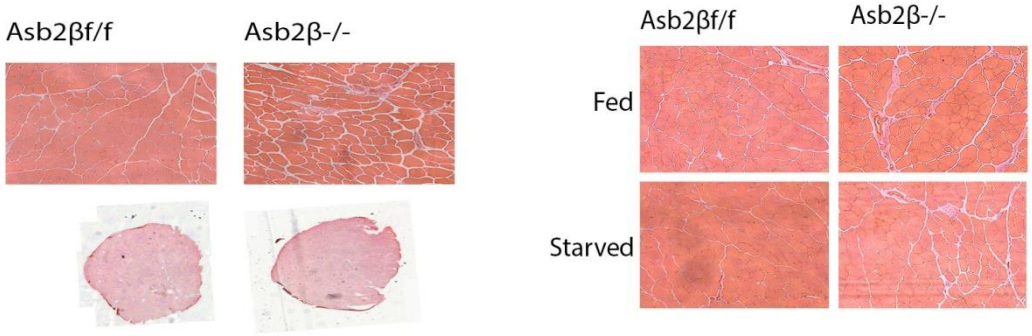

Image 13: H/E staning where we can see the difference in the stracture between the Asb2β -/- and Asb2β f/f mice.

We observed the presence of degenerated and necrotic muscle fibers, positive for IgG staining (in green),(image), together with abnormal mitochondrial distribution in fed conditions of knock-out mice muscles.

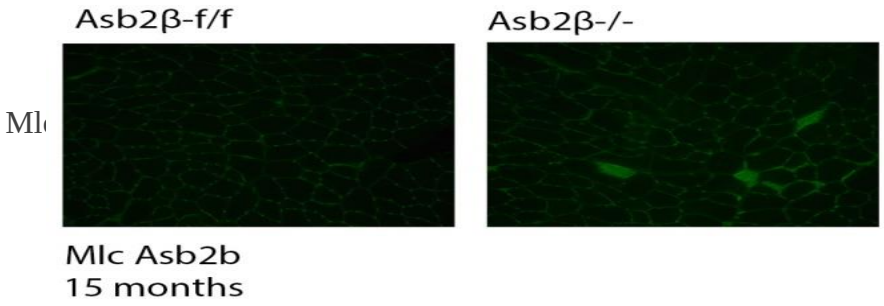

Image 14: IgG staining where we can observe the IgG positive fibers in the Asb2β-/- mice.

Moreover, we analyze the size of both oxidative and glycolytic muscle fibers and we observed a significant difference only in the oxidative fibers between the controls and the knock out mice.

These findings suggest that a long- term deletion of Asb2β probably leads to a fasting-like condition that could be detrimental for muscle function. It unravels Asb2β as a gene central for energy homeostasis in skeletal muscles.

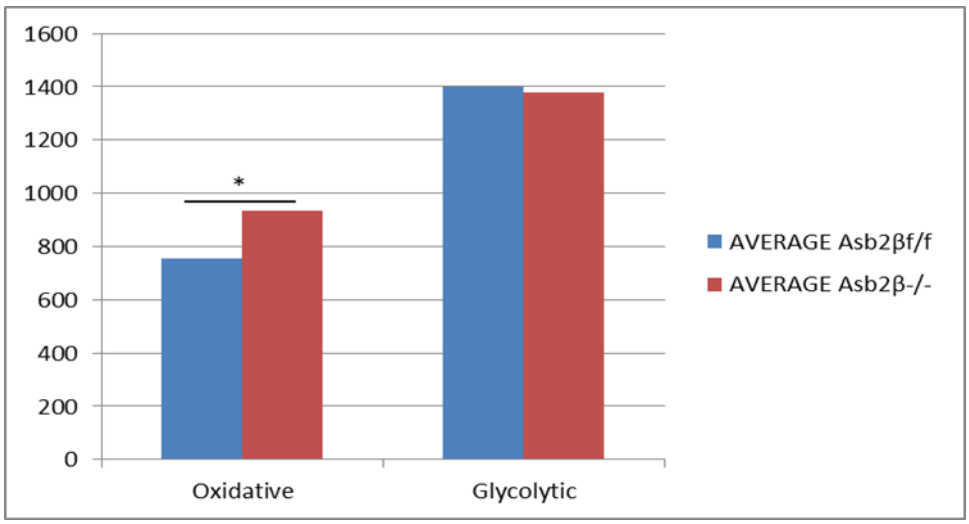

Image 16: Diagram of the glycolytic and oxidative fiber size.The analysis showed a significant difference of the oxidative fiber size (bigger fibers in the KOs), but not in the glycolytic ones. Data present mean + s.e.m (*, p< 0,05).

To identify if there is any fiber loss, we analyze the size of the controls and the K.O Asb2β animals.

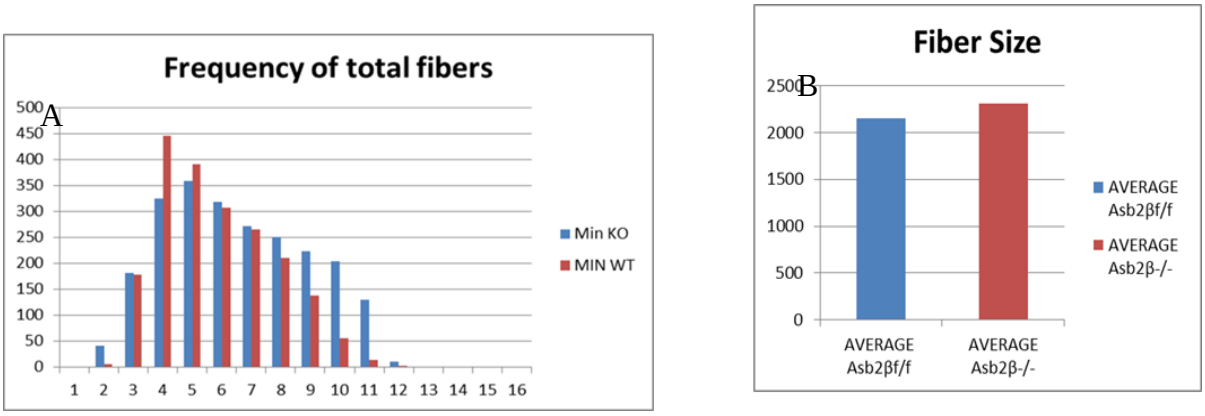

Image 15: A) Diagram of the frequency histograms of tibialis muscles showing the distribution of cross-sectional areas (mm2) of inducible Asb2β muscle specific mice after where we can observe that the most fibers of the KO mice have a medium size, and we can observe the difference comparing to the controls. B) Diagram of the average size (μm2) of the controls and the KO mice where there is an insignificant trend for the Kos to have bigger fibers.

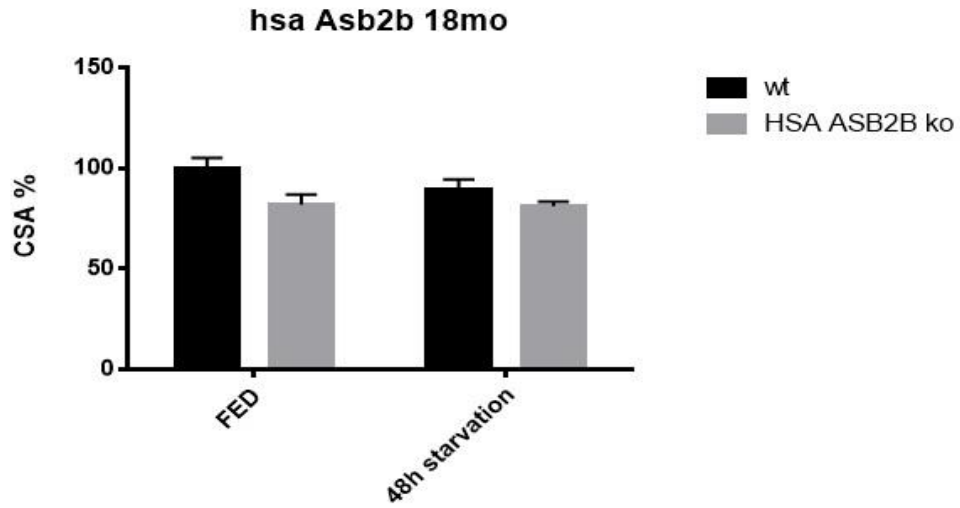

Image 17: Diagram comparing the average size of controls and KO mice in Fed and starve conditions. There is no significant difference

The results showed that there is a trend of the K.O mice to have larger fibers but when considerind oxidative nad glycolytic fibers all togeather the difference from the controls is not significant. .

Since we want to figure out if Asb2βs might be an important regulator of energy metabolism in muscle and if it is important for glucose homeostasis in the liver, we decided to monitor glycogen levels. PAS staining revealed that here is a different distribution of glycogen stores in muscle. In controls we can see slightly more intense color than the one in Asb2β knock-out mice. Of course in starvation

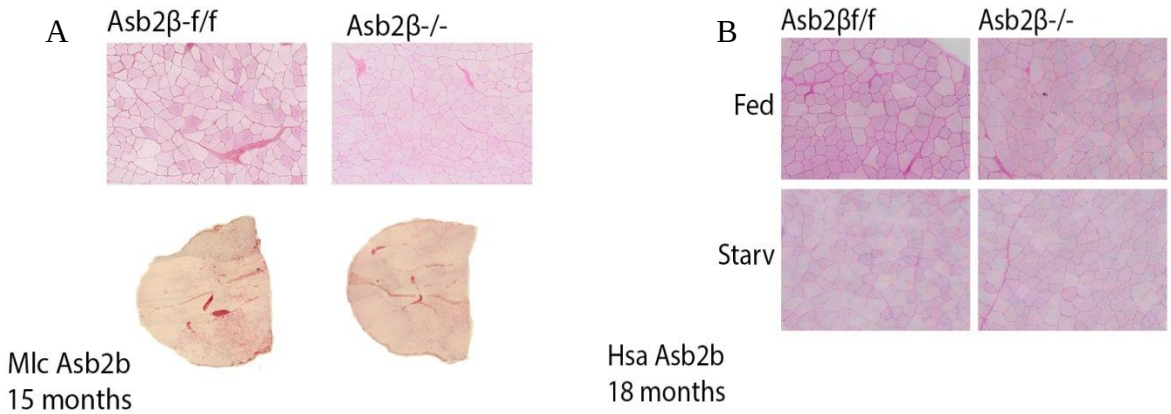

Image 18: A) Images from PAS staining where we can observe that KO mice have less glycogen stored in the muscle fibers. B) Images of PAS staining where we can compare the mice in Fed and starve conditions. We can see that after starvation the glycogen is almost disappeared from the fibers.

condition the glycogen storage is almost empty in the muscle fibers.

Since other muscle-specific E3s, such as Atrogin1 and MuRF1, are central for the turnover of glucose metabolic key enzymes (Hirner et al., 2008; Lokireddy et al.,

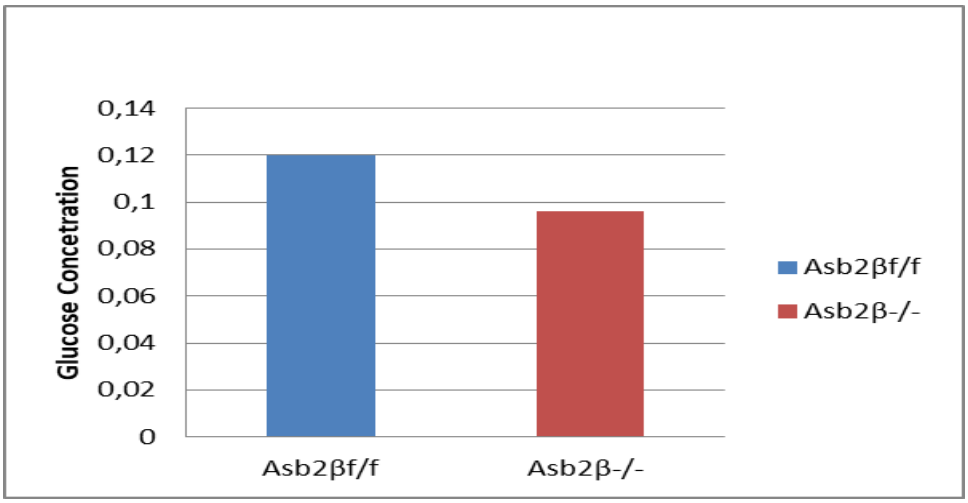

Image 19: Diagram of the glycogen assay. We observed an insignificant trend of the KO mice to have less glycogen stored in the muscle fibers.

2012), we wondered whether Asb2β has a role in carbohydrate metabolism. Therefore, we monitored glycogen levels in muscles. In basal conditions, KO muscle glycogen stores levels were slightly lower in knockout muscles.

Moreover, to investigate if there are in vivo abnormalities in the glucose metabolism we performed the Glucose tolerance test (GTT), the Insulin tolerance test (ITT) and the Pyruvate tolerance test (PTT) in another group of 18 month old mice.

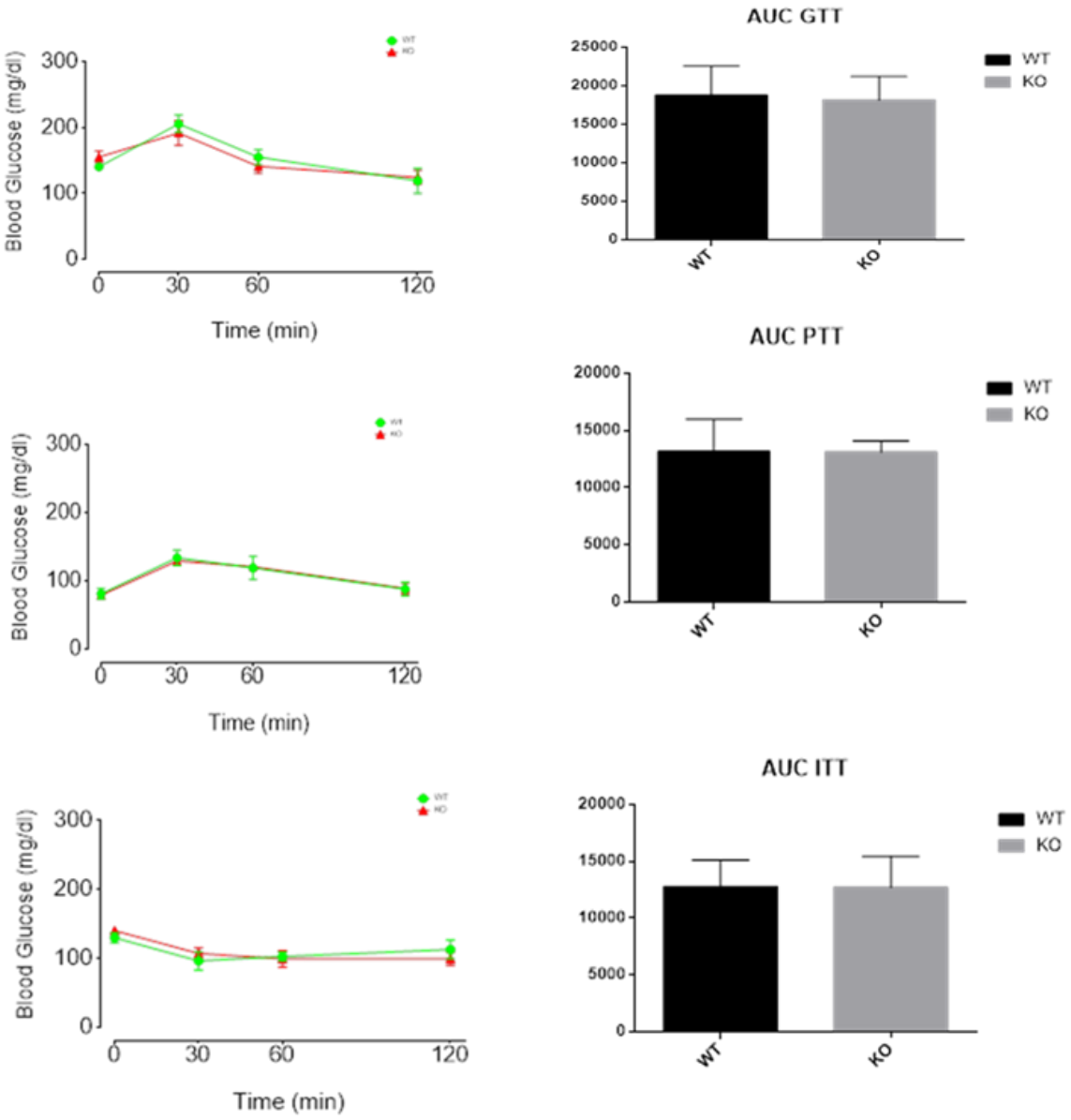

Image 20: A) Diagram of the analysis of the GTT test. B) Diagram of the data analysis of the PTT test. C) Diagream of the data analysis of the ITT test. There are no differenses in any of the tests.

We observe no differences in any of the three tolerance experiments.

3.3. Asb2β-null muscles have alterations in mitochondrial distribution

SDH staining showed some alterations in the distribution muscle mitochondria both in the Asb2β-/- mice in both, the conditional and the inducible model.

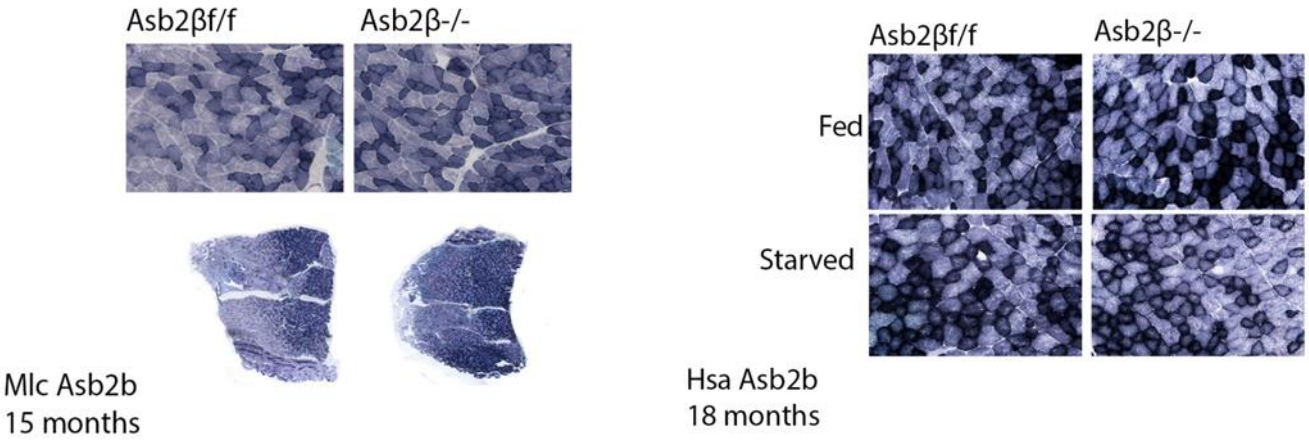

Image 21: Pictures of SDH staining. We can observe the different mitochondrial distribution between the controls and the Ko mice in also fed and starve conditions.

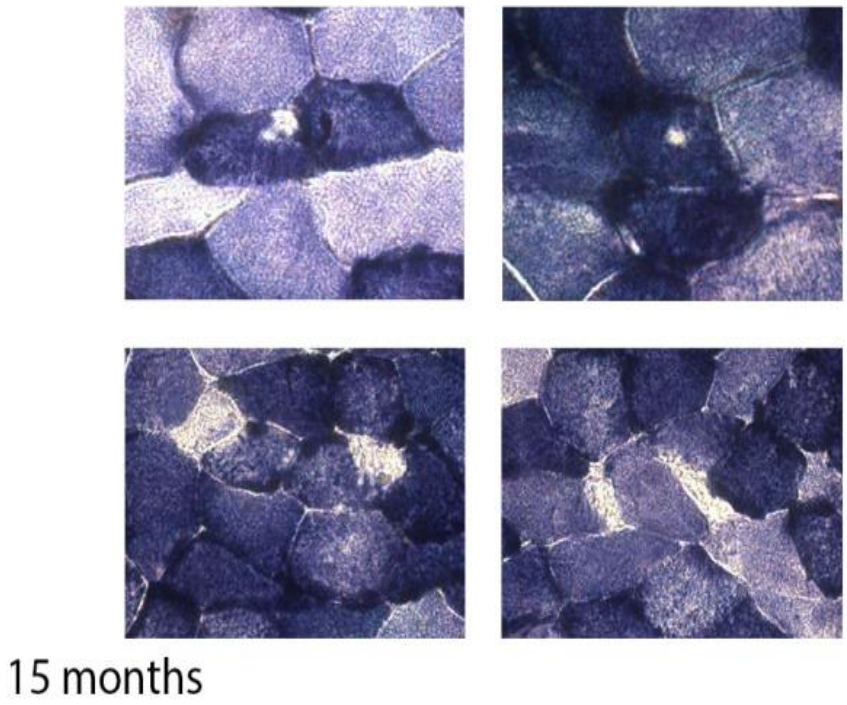

Image 22: Pictures of SDH staining in 40x focus. Optical observation of mitochondrial alterations.

Since there are alterations in the mitochondrial distribution, we decided to check mitochondrial quality control via the measurement of the fission mediator Drp1, as

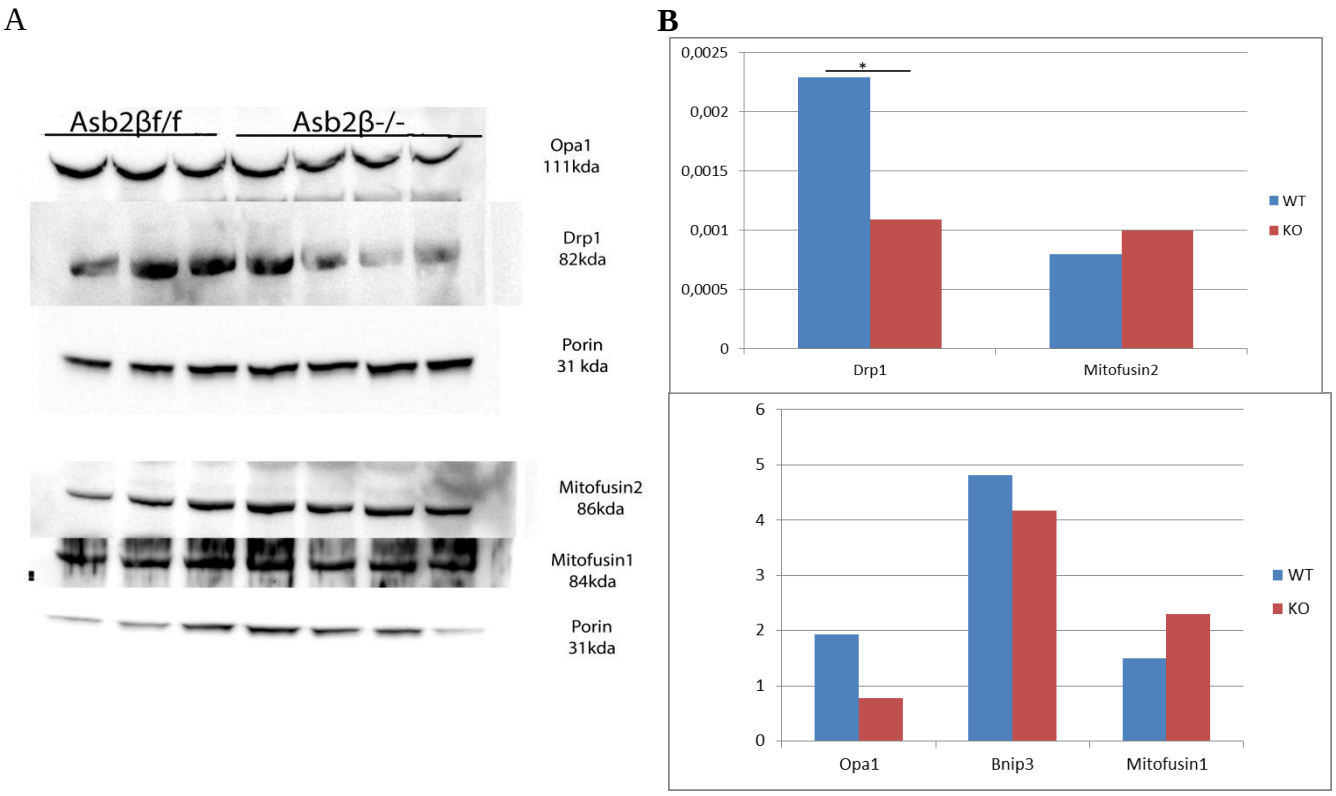

Image 23: A) WB analysis of Opa1, Drp1, Mitofusin 1&2. B) Diagram of WB analysis. The only protein that had a significant difference was the fission mediator Drp1, where the KO mice had a dowrwgulation of the protein.

well as the fusion mediators Mfn1 and 2 and OPA1 (Westermann et all., 2008). The results showed that there are not significant differences except from the fission mediator Drp1, where we see a significant difference between the controls and the knock-out mice. Dynamin-related protein 1 is a large GTPase, mediates mitochondrial fission in mammalian cells (Okamoto and Shaw 2005; Hoppins et al. 2007). That means that the fission is upregulated in Asb2β knock-out mice.

Then, we checked the activation of the oxidative stress pathways by measuring the carbonylation of the muscle proteins. An oxyblot revealed a non-significant difference between wild type and Asb2β knockout mice.

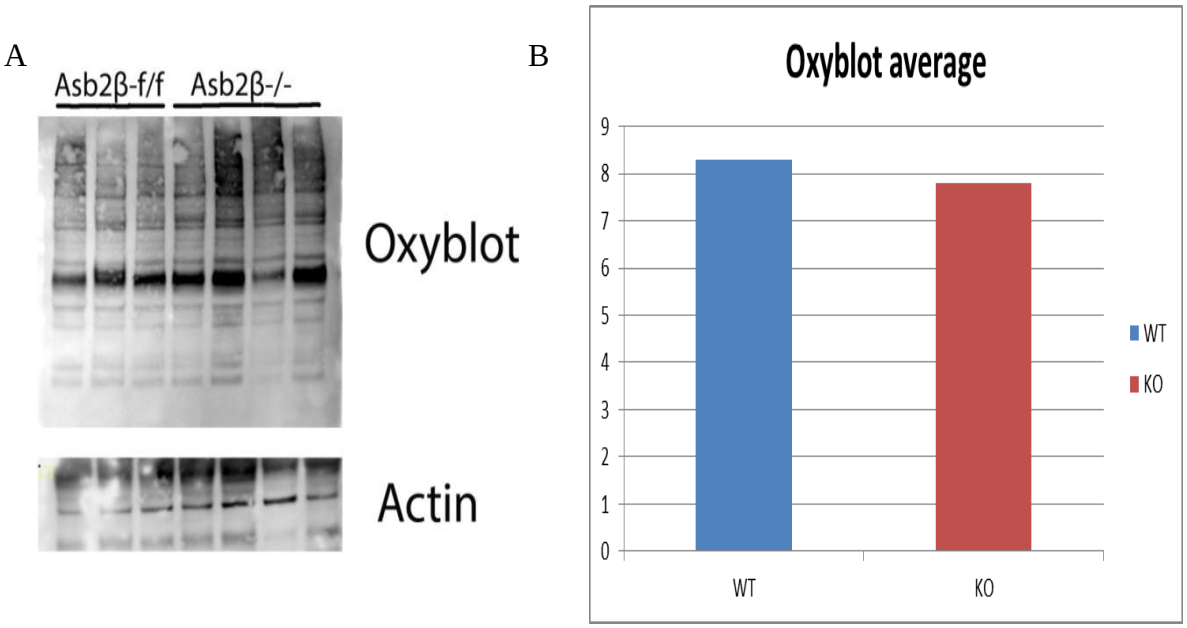

Image 24 : A) Oxyblot analysis. B) Diagram of the oxyblot analysis where there are no significant diferences between the controls and the KO mice for the oxydative stress proteins.

We also performed the exhaustion experiment in order to perceive if there are any differences on the physical performance of the animals. We compered the distance (meters) and the time (min) that the Asb2βf/f and the Asb2β-/- run via the Treadmill test. From the analysis of the data, it comes out a trend where the controls are more

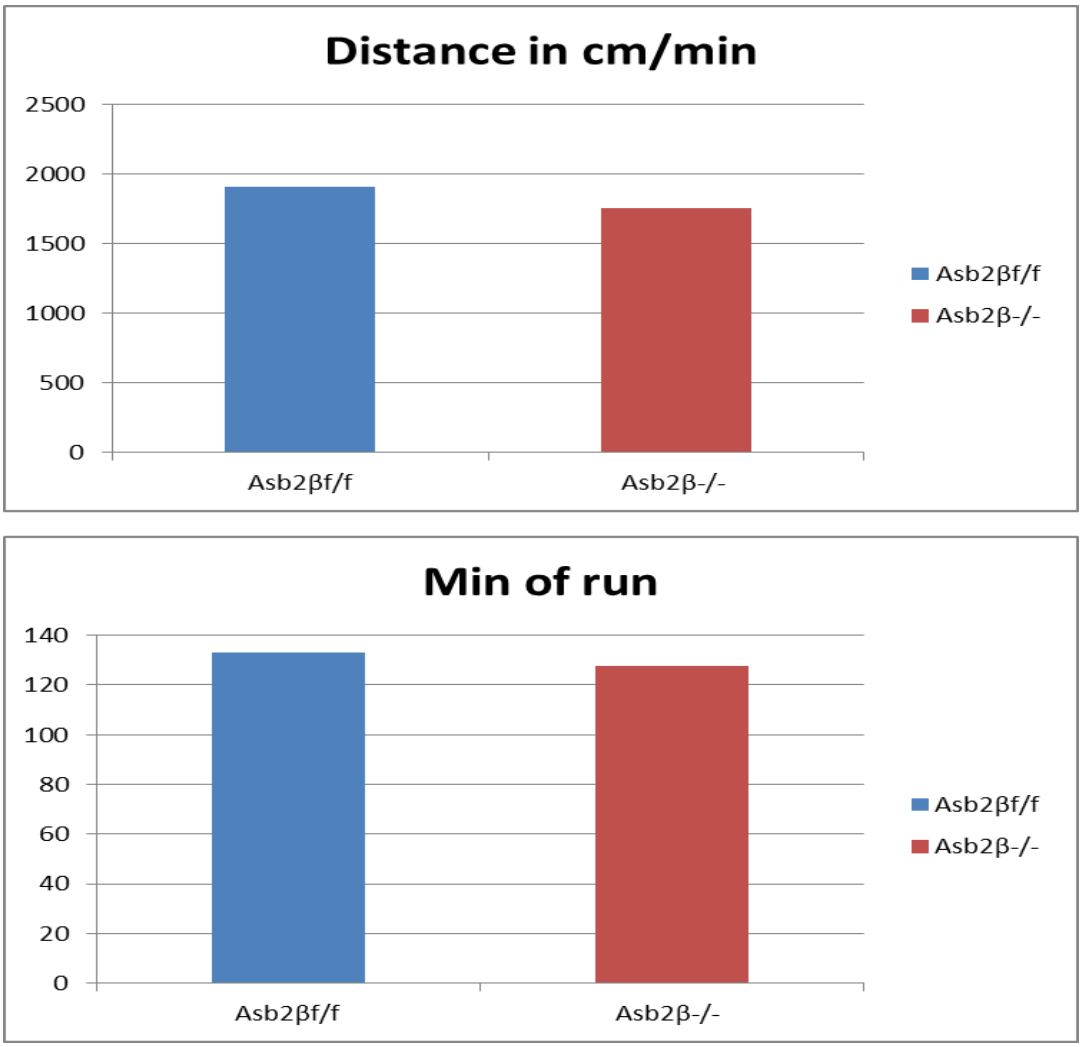

Image 25: Diagram of the exhaustion experiment where there is no difference on the performance both of KO and control mice.

resistant on physical activity than the knock-out mice. However, the differences are small and not significant both in the distance and the time of the physical activity.

4 Discussion

Muscle atrophy occurs in specific muscles with denervation or inactivity, but is also a systemic response to fasting and various diseases. The identification of the precise signaling cascades that regulate muscle wasting remains poorly understood.

The Ubiquitin Proteasome System (UPS) is one of the major mechanism that control proteolysis and, ubiquitination of protein substrates, occurs through the sequential action of distinct enzymes: E1 (ubiquitin-activating enzyme), E2 (ubiquitin-conjugating enzyme) and E3 (ubiquitin-protein-ligase). The rate-limiting step of the ubiquitination process depends on hundreds of E3s, that recognize specific substrates. Characterization of the E3s and of their respective targets in skeletal muscle atrophy is an important step to understand the mechanisms that control muscle mass and to further develop pharmacological interventions in muscle disease. Ankyrin repeat and SOCS box containing 2 beta (Asb2β), one on the two transcript variants of the ASB2 gene, is a novel muscle-specific E3 ubiquitin ligase that regulates muscle differentiation [87].

Among the hundreds of E3 ubiquitin ligases, only few have been found to regulate muscle mass. In addition to MuRF1 and Atrogin1 (also known as Fbxo32), we recently identified other two novel FoxO-dependent E3 ligases, that we named SMART (also known as Fbxo21) and MUSA1 (also known as Fbxo30) (Milan et al., 2015). Atrogin-1, MuRF1, MUSA1 and SMART are E3s strongly upregulated in different catabolic conditions [89], [90], [91]. Knockdown of either one of these genes partially protects from muscle atrophy [89], [90], [91], [100]. Interestingly, the overexpression in muscles of Asb2β, and not of the other E3 ligases, Atrogin1, MuRF1 or MUSA1, is sufficient to induce muscle atrophy [98], [99], [100]. However, how, Asb2β activates an atrophy program and which are its specific substrates are unexplored issues. According to the literature, Asb2β is a novel regulator of muscle mass because Asb2β is a TGF-β network-responsive negative regulator of muscle mass [98] and reduced levels of Asb2β are associated with hypertrophic cardiomyopathy [101].

In addition, Asb2β is a circadian gene, which might control rate-limiting steps in metabolic pathways to prepare the organism for daily environmental changes [102].

Interestingly, chronic disruption of circadian clocks components has consistently been linked to metabolic disorders and diseases. Taken together, Asb2β is a very attractive candidate to investigate metabolic changes in skeletal muscle mass regulation.

This work is based on the study of the role of Asb2β in vivo, a new E3 muscle-specific ubiquitin ligase. To understand its role, we have generated skeletal muscle specific knock-out mouse models and we analyzed its function in physiological and in muscle wasting conditions. Asb2β defective muscles show normal muscle architecture but, interestingly, we observe that these mice are hypoglycemic and display an accumulation of glycogen stores. Since glycogen represents the main energy source in muscle in catabolic conditions, we decided to use starvation as muscle atrophy model. Starved knock-out muscle fibers are necrotic, morphologically altered with abnormal mitochondrial distribution. Another interesting observation is that the fibers appeared completely deprived of glycogen stores, suggesting that the lack of Asb2β could be important to maintain a functional homeostasis during catabolic conditions.

Our preliminary findings provide the first evidence of the involvement of Asb2β in the control of muscle mass and regulation of glucose metabolism in skeletal muscle. Furthermore, characterization of different E3s and their respective substrates in skeletal muscle could represent an important step to understand the mechanisms that control muscle mass loss and, moreover, to develop targets for pharmacological intervention in muscle disease.

.

Summary

Atrophy is an active process controlled by specific signaling pathways and transcriptional programs but the identification of the precise signaling cascades that direct muscle wasting remains poorly understood. The Ubiquitin Proteasome System (UPS) is one of the major mechanisms that control proteolysis and ubiquitination of protein substrates. The specificity of ubiquitin-dependent degradation derives from many E3s that recognize specific substrates. This work is based on the study of the role of Asb2β in vivo, a new E3 muscle-specific ubiquitin ligase. To understand its role, we have generated skeletal muscle specific knock-out mouse models and we analyzed its function in physiological and in muscle wasting conditions. Asb2β defective muscles show normal muscle architecture but, interestingly, we observe that these mice display an accumulation of glycogen stores. Since glycogen represents the main energy source in muscle in catabolic conditions, we decided to use starvation as muscle atrophy model. Starved knock-out muscle fibers are necrotic, morphologically altered and with abnormal mitochondrial distribution. Another interesting observation is that the fibers appeared completely deprived of glycogen stores, suggesting that the lack of Asb2β could be important to maintain a functional homeostasis during catabolic conditions. Moreover, skeletal muscle inducible model results in muscle hypertrophy. Our preliminary findings provide the first evidence of the involvement of Asb2β in the control of muscle mass and regulation of glucose metabolism in skeletal muscle. Furthermore, characterization of different E3s and their respective substrates in skeletal muscle could represent an important step to understand the mechanisms that control muscle mass loss and, moreover, to develop targets for pharmacological intervention in muscle disease

References

1 Skeletal Muscle Structure, Function, and Plasticity; Richard L. Lieber :Lippincott Williams & Wilkins, 2002

2 Pette D., Heilmann C. (1979). Some characteristics of sarcoplasmic reticulum in fast- and slow-twitch muscles. Biochem Soc Trans. 7, 765-767.

3 Schiaffino S., Sandri M., Murgia M. (2007). Activity-dependent signaling pathways controlling muscle diversity and plasticity. Physiology (Bethesda). 22, 269-278.

4 Ciciliot S., Rossi A.C., Dyar K.A., Blaauw B., Schiaffino S. (2013). Muscle type and fiber type specificity in muscle wasting. Int. J. Biochem. Cell Biol. 45, 21912199.

5 Schiaffino S., Reggiani C. (2011). Fiber types in mammalian skeletal muscles. Physiol Rev. 91, 1447-1531.

6 Schiaffino S., Reggiani C. (1996). Molecular diversity of myofibrillar proteins: gene regulation and functional significance. Physiol Rev. 76, 371-423.

7 Murgia M., Serrano A.L., Calabria E., Pallafacchina G., Lomo T., Schiaffino S. (2000). Ras is involved in nerve-activity-dependent regulation of muscle genes. Nat Cell Biol. 2, 142-147.

8 Schiaffino S., Dyar K.A., Ciciliot S., Blaauw B., Sandri M. (2013). Mechanisms regulating skeletal muscle growth and atrophy. FEBS J. 280, 4294-4314.

9 Lee Y.J., Jeong S.Y., Karbowski M., Smith C.L., and Youle R.J. (2004). Roles of the mammalian mitochondrial fission and fusion mediators Fis1, Drp1, and Opa1 in apoptosis. Mol. Biol. Cell. 15, 5001-5011.

10 Sartori R., Schirwis E., Blaauw B., Bortolanza S., Zhao J., Enzo E., Stantzou A., Mouisel E., Toniolo L., Ferry A., Stricker S., Goldberg A.L., Dupont S., Piccolo S., Amthor H., Sandri M. (2013). BMP signaling controls muscle mass. Nat Genet. 45, 1309-1318

11 Lecker S.H., Jagoe R.T., Gilbert A., Gomes M., Baracos V., Bailey J., Price S.R., Mitch W.E., Goldberg A.L. (2004). Multiple types of skeletal muscle atrophy involve a common program of changes in gene expression. FASEB J. 18, 39-51.

12 Sandri M. (2013). Protein breakdown in muscle wasting: role of autophagylysosome and ubiquitin-proteasome. Int. J. Biochem. Cell Biol. 45, 2121-2129.

13 Mizushima N., and Komatsu M. (2011). Autophagy: renovation of cells and tissues. Cell 147, 728-741.

14 Shintani, T., and Klionsky, D. J. (2004a). Autophagy in health and disease: a double-edged sword. Science 306, 990-995.

15 Kamura T, Koepp DM, Conrad MN, Skowyra D, Moreland RJ, Iliopoulos O, Lane WS, Kaelin WG, Elledge SJ, Conaway RC, Harper JW, Conaway JW (1999). Rbx1, a component of the VHL tumor suppressor complex and SCF ubiquitin ligase. Science 284(5414):657-61

16 Mizushima N., and Komatsu M. (2011). Autophagy: renovation of cells and tissues. Cell 147, 728-741.

17 Lum, J.J., D.E. Bauer, M. Kong, M.H. Harris, C. Li, T. Lindsten, and C.B. Thompson. 2005. Growth factor regulation of autophagy and cell survival in the absence of apoptosis. Cell. 120:237–248.

18 Mordier S, Deval C, Bechet D, et al. Leucine limitation induces autophagy and activation of lysosome-dependent proteolysis in C2C12 myotubes through a mammalian target of rapamycin-independent signaling pathway. J Biol Chem. 2000;275:29900–6.

19 Koch, D., G.A. Schmidt, and C.V. Field, 2006: Sulfur, sea salt and radionuclide aerosols in GISS ModelE. J. Geophys. Res., 111, D06206, doi:10.1029/2004JD005550.

20 Sarkar AK1, Luijten M, Miyashima S, Lenhard M, Hashimoto T, Nakajima K, Scheres B, Heidstra R, Laux T. Conserved factors regulate signalling in Arabidopsis thaliana shoot and root stem cell organizers. Nature. 2007 Apr 12;446(7137):811-4.

21 Yamamoto A, Mizushima N, Tsukamoto S. Fertilization-induced autophagy in mouse embryos is independent of mTORC1. Biol Reprod. 2014;91:7.

22 Sacheck JM, Hyatt JP, Raffaello A, Jagoe RT, Roy RR, Edgerton VR, Lecker SH, Goldberg AL. Rapid disuse and denervation atrophy involve transcriptional changes similar to those of muscle wasting during systemic diseases. FASEB J. 2007;21:140–155.

23 Lecker SH, Jagoe RT, Gilbert A, Gomes M, Baracos V, Bailey J, Price SR, Mitch WE, Goldberg AL. Multiple types of skeletal muscle atrophy involve a common program of changes in gene expression. FASEB J. 2004;18:39–51.

24 Juhasz G, Erdi B, Sass M, Neufeld TP. Atg7-dependent autophagy promotes neuronal health, stress tolerance, and longevity but is dispensable for metamorphosis in Drosophila. Genes Dev. 2007;21:3061–6.

25 Mammucari C, Milan G, Romanello V, Masiero E, Rudolf R, Del Piccolo P, Burden SJ, Di Lisi R, Sandri C, Zhao J, et al. FoxO3 controls autophagy in skeletal muscle in vivo. Cell Metab. 2007;6:458–471.

26 Glickman MH, Ciechanover A. The ubiquitin-proteasome proteolytic pathway: destruction for the sake of construction. Physiol Rev. 2002;82:373–428

27 Rotin D., Kumar S. (2009). Physiological functions of the HECT family of ubiquitin ligases. Nat. Rev. Mol. Cell Biol. 10, 398-409

28 Huang L., Kinnucan E., Wang G., Beaudenon S., Howley P. M., Huibregtse J. M., Pavletich N. P. (1999). Structure of an E6AP-UbcH7 complex: insights into ubiquitination by the E2-E3 enzyme cascade. Science 286, 1321-1326

29 Kamadurai H. B., Souphron J., Scott D. C., Duda D. M., Miller D. J., Stringer D., Piper R. C., Schulman B. A. (2009). Insights into ubiquitin transfer cascades from a structure of a UbcH5B approximately ubiquitin-HECT(NEDD4L) complex. Mol. Cell 36, 1095-1102

30 Huibregtse J. M., Scheffner M., Beaudenon S., Howley P. M. (1995). A family of proteins structurally and functionally related to the E6-AP ubiquitin-protein ligase. Proc. Natl. Acad. Sci. USA 92, 2563-2567

31 Huang L., Kinnucan E., Wang G., Beaudenon S., Howley P. M., et al. , 1999. Structure of an E6AP-UbcH7 complex: insights into ubiquitination by the E2–E3 enzyme cascade. Science 286: 1321–1326

32 Ogunjimi A. A., Briant D. J., Pece-Barbara N., Le Roy C., Di Guglielmo G. M., Kavsak P., Rasmussen R. K., Seet B. T., Sicheri F., Wrana J. L. (2005). Regulation of Smurf2 ubiquitin ligase activity by anchoring the E2 to the HECT domain. Mol. Cell 19, 297-308

33 Verdecia M. A., Joazeiro C. A., Wells N. J., Ferrer J. L., Bowman M. E., Hunter T., Noel J. P. (2003). Conformational flexibility underlies ubiquitin ligation mediated by the WWP1 HECT domain E3 ligase. Mol. Cell 11, 249-259

34 Kim H. C., Huibregtse J. M. (2009). Polyubiquitination by HECT E3s and the determinants of chain type specificity. Mol. Cell. Biol. 29, 3307-3318

35 Li JY, Chai B, Zhang W, Wu X, Zhang C, Fritze D, Xia Z, Patterson C, Mulholland MW. Ankyrin repeat and SOCS box containing protein 4 (Asb-4) colocalizes with insulin receptor substrate 4 (IRS4) in the hypothalamic neurons and mediates IRS4 degradation. BMC Neurosci. 2011;12:95.

36 Lorick K. L., Jensen J. P., Fang S., Ong A. M., Hatakeyama S., Weissman A. M. (1999). RING fingers mediate ubiquitin-conjugating enzyme (E2)-dependent ubiquitination. Proc. Natl. Acad. Sci. USA 96, 11364-11369

37 Zheng N., Wang P., Jeffrey P. D., Pavletich N. P. (2000). Structure of a c-Cbl-UbcH7 complex: RING domain function in ubiquitin-protein ligases. Cell 102,

38 Ozkan E., Yu H., Deisenhofer J. (2005). Mechanistic insight into the allosteric activation of a ubiquitin-conjugating enzyme by RING-type ubiquitin ligases. Proc. Natl. Acad. Sci. USA 102, 18890-18895

39 Liew C. W., Sun H., Hunter T., Day C. L. (2010). RING domain dimerization is essential for RNF4 function. Biochem. J. 431, 23-29

40 Mace P. D., Linke K., Feltham R., Schumacher F. R., Smith C. A., Vaux D. L., Silke J., Day C. L. (2008). Structures of the cIAP2 RING domain reveal conformational changes associated with ubiquitin-conjugating enzyme (E2) recruitment. J. Biol. Chem. 283, 31633-31640

41 Polekhina G., House C. M., Traficante N., Mackay J. P., Relaix F., Sassoon D. A., Parker M. W., Bowtell D. D. (2002). Siah ubiquitin ligase is structurally related to TRAF and modulates TNF-alpha signaling. Nat. Struct. Biol. 9, 68-75

42 Park Y. C., Burkitt V., Villa A. R., Tong L., Wu H. (1999). Structural basis for self-association and receptor recognition of human TRAF2. Nature 398, 533-538

43 Brzovic P. S., Rajagopal P., Hoyt D. W., King M. C., Klevit R. E. (2001). Structure of a BRCA1-BARD1 heterodimeric RING-RING complex. Nat. Struct. Biol. 8, 833-837

44 Buchwald G., van der Stoop P., Weichenrieder O., Perrakis A., van Lohuizen M., Sixma T. K. (2006). Structure and E3-ligase activity of the Ring-Ring complex of polycomb proteins Bmi1 and Ring1b. EMBO J. 25, 2465-2474

45 Linke K., Mace P. D., Smith C. A., Vaux D. L., Silke J., Day C. L. (2008). Structure of the MDM2/MDMX RING domain heterodimer reveals dimerization is required for their ubiquitylation in trans. Cell Death Differ. 15, 841-848

46 Satijn D. P., Otte A. P. (1999). RING1 interacts with multiple Polycomb-group proteins and displays tumorigenic activity. Mol. Cell. Biol. 19, 57-68

47 Simons A. M., Horwitz A. A., Starita L. M., Griffin K., Williams R. S., Glover J. N., Parvin J. D. (2006). BRCA1 DNA-binding activity is stimulated by BARD1. Cancer Res. 66, 2012-2018

48 Sharp D. A., Kratowicz S. A., Sank M. J., George D. L. (1999). Stabilization of the MDM2 oncoprotein by interaction with the structurally related MDMX protein. J. Biol. Chem. 274, 38189-38196

49 Wu L. C., Wang Z. W., Tsan J. T., Spillman M. A., Phung A., Xu X. L., Yang M. C., Hwang L. Y., Bowcock A. M., Baer R. (1996). Identification of a RING protein that can interact in vivo with the BRCA1 gene product. Nat. Genet. 14, 430-440

50 Hua Z., Vierstra R. D. (2011). The cullin-RING ubiquitin-protein ligases. Annu. Rev. Plant Biol. 62, 299-334

51 Petroski M. D., Deshaies R. J. (2005). Function and regulation of cullin-RING ubiquitin ligases. Nat. Rev. Mol. Cell Biol. 6, 9

52 Kohroki J1, Nishiyama T, Nakamura T, Masuho Y. ASB proteins interact with Cullin5 and Rbx2 to form E3 ubiquitin ligase complexes. FEBS Lett. 2005 Dec 19;579(30):6796-802. Epub 2005 Nov 28.

53 Andresen CA, Smedegaard S, Sylvestersen KB, Svensson C, Iglesias-Gato D, Cazzamali G, Nielsen TK, Nielsen ML, Flores-Morales A. Protein interaction screening for the ankyrin repeats and suppressor of cytokine signaling (SOCS) Box (ASB) family identify Asb11 as a novel endoplasmic reticulum resident ubiquitin ligase. J Biol Chem. 2014;289:2043–54

54 Guibal FC, Moog-Lutz C, Smolewski P, Di Gioia Y, Darzynkiewicz Z, Lutz PG, Cayre YE. ASB-2 inhibits growth and promotes commitment in myeloid leukemia cells. J Biol Chem. 2002;277:218–24.

55 Heuze ML, Lamsoul I, Baldassarre M, Lad Y, Leveque S, Razinia Z, Moog-Lutz C, Calderwood DA, Lutz PG. ASB2 targets filamins A and B to proteasomal degradation. Blood. 2008;112:5130–40.

56 Lamsoul I, Erard M, van der Ven PFM, Lutz PG. Filamins but not janus kinases are substrates of the ASB2 alpha cullin-ring E3 ubiquitin ligase in hematopoietic cells. PLoS One. 2012;7:e43798.

57 Razinia Z, Baldassarre M, Cantelli G, Calderwood DA. ASB2alpha, an E3 ubiquitin ligase specificity subunit, regulates cell spreading and triggers proteasomal degradation of filamins by targeting the filamin calponin homology 1 domain. J Biol Chem. 2013;288:32093–105.

58 Heuze ML, Lamsoul I, Baldassarre M, et al. ASB2 targets filamins A and B to proteasomal degradation. Blood. 2008;112(13):5130-5140

59 Lamsoul I, Burande CF, Razinia Z, Houles TC, Menoret D, Baldassarre M, Erard M, Moog-Lutz C, Calderwood DA, Lutz PG. Functional and structural insights into ASB2 alpha, a novel regulator of integrin-dependent adhesion of hematopoietic cells. J Biol Chem. 2011;286:30571–81.

60 Spinner CA, Uttenweiler-Joseph S, Metais A, Stella A, Burlet-Schiltz O, Moog-Lutz C, Lamsoul I, Lutz PG. Substrates of the ASB2 alpha E3 ubiquitin ligase in dendritic cells. Sci Rep Uk. 2015;5.

61 Chung AS, Guan YJ, Yuan ZL, Albina JE, Chin YE. Ankyrin repeat and SOCS box 3 (ASB3) mediates ubiquitination and degradation of tumor necrosis factor receptor II. Mol Cell Biol. 2005;25:4716–26.

62 Fantin VR, Lavan BE, Wang Q, Jenkins NA, Gilbert DJ, Copeland NG, Keller SR, Lienhard GE. Cloning, tissue expression, and chromosomal location of the mouse insulin receptor substrate 4 gene. Endocrinology. 1999;140:1329–37.

63 Numan S, Russell DS. Discrete expression of insulin receptor substrate-4 mRNA in adult rat brain. Mol Brain Res. 1999;72:97–102.

64 Au V, Tsang FH, Man K, Fan ST, Poon RTP, Lee NP. Expression of ankyrin repeat and SOCS box containing 4 (ASB4) confers migration and invasion properties of hepatocellular carcinoma cells. Biosci Trends. 2014;8:101–10.

65 Wang H, Charles PC, Wu YX, Ren RQ, Pi XC, Moser M, Barshishat-Kupper M, Rubin JS, Perou C, Bautch V, et al. Gene expression profile signatures indicate a role for Wnt signaling in endothelial commitment from embryonic stem cells. Circ Res. 2006;98:1331–9.

66 Ferguson JE, Wu Y, Smith K, Charles P, Powers K, Wang H, Patterson C. ASB4 is a hydroxylation substrate of FIH and promotes vascular differentiation via an oxygen-dependent mechanism. Mol Cell Biol. 2007;27:6407–19.

67 Janatpour MJ, McMaster MT, Genbacev O, Zhou Y, Dong JY, Cross JC, Israel MA, Fisher SJ. Id-2 regulates critical aspects of human cytotrophoblast differentiation, invasion and migration. Development. 2000;127:549–58.

68 Lasorella A, Rothschild G, Yokota Y, Russell RG, Iavarone A. Id2 mediates tumor initiation, proliferation, and angiogenesis in Rb mutant mice. Mol Cell Biol. 2005;25:3563–74.

69 Townley-Tilson WHD, Wu YX, Ferguson JE, Patterson C. The ubiquitin ligase ASB4 promotes trophoblast differentiation through the degradation of ID2. PLoS One. 2014;9:e89451.

70 Wilcox A, Katsanakis KD, Bheda F, Pillay TS. Asb6, an adipocyte-specific ankyrin and SOCS box protein, interacts with APS to enable recruitment of elongins B and C to the insulin receptor signaling complex. J Biol Chem. 2004;279:38881–8.

71 Fei XW, Gu X, Fan SL, Yang ZX, Li F, Zhang C, Gong WM, Mao YM, Ji CN. Crystal structure of human ASB9-2 and substrate-recognition of CKB. Protein J. 2012;31:275–84.

72 Fei XW, Zhang Y, Gu X, Qiu R, Mao YM, Ji CN. Crystallization and preliminary X-Ray analysis of the splice variant of human ankyrin repeat and suppressor of cytokine signaling box protein 9 (hASB9-2). Protein Peptide Lett. 2009;16:333–5.

73 Muniz JR, Guo K, Kershaw NJ, Ayinampudi V, von Delft F, Babon JJ, Bullock AN. Molecular architecture of the ankyrin SOCS box family of Cul5-dependent E3 ubiquitin ligases. J Mol Biol. 2013;425:3166–77.

74 Thomas JC, Matak-Vinkovic D, Van Molle I, Ciulli A. Multimeric complexes among ankyrin-repeat and SOCS-box protein 9 (ASB9), ElonginBC, and cullin 5: insights into the structure and assembly of ECS-type cullin-RING E3 ubiquitin ligases. Biochem Us. 2013;52:5236–46.

75 Balasubramaniam D, Schiffer J, Parnell J, Mir SP, Amaro RE, Komives EA. How the ankyrin and SOCS box protein, ASB9, binds to creatine kinase. Biochem Us. 2015;54:1673–80.

76 Kwon S, Kim D, Rhee JW, Park JA, Kim DW, Kim DS, Lee Y, Kwon HJ. ASB9 interacts with ubiquitous mitochondrial creatine kinase and inhibits mitochondrial function. Bmc Biol. 2010;8:1.

77 Kwon S, Kim D, Rhee JW, Park JA, Kim DW, Kim DS, Lee Y, Kwon HJ. ASB9 interacts with ubiquitous mitochondrial creatine kinase and inhibits mitochondrial function. Bmc Biol. 2010;8:1.

78 Wyss M, Kaddurah-Daouk R. Creatine and creatinine metabolism. Physiol Rev. 2000;80:1107–213.

79 Wallimann T, Hemmer W. Creatine kinase in non-muscle tissues and cells. Mol Cell Biochem. 1994;133–134:193–220.

80 Lai E. C. (2004). Notch signaling: control of cell communication and cell fate. Development 131, 965–97310.1242/dev.01074

81 Louvi A, Artavanis-Tsakonas S. Notch signalling in vertebrate neural development. Nat Rev Neurosci. 2006;7:93–102.

82 Mumm JS, Kopan R. Notch signaling: from the outside in. Dev Biol. 2000;228:151–65.

83 Diks SH, Bink RJ, van de Water S, Joore J, van Rooijen C, Verbeek FJ, den Hertog J, Peppelenbosch MP, Zivkovic D. The novel gene asb11: a regulator of the size of the neural progenitor compartment. J Cell Biol. 2006;174:581–92.

84 Diks SH, da Silva MAS, Hillebrands JL, Bink RJ, Versteeg HH, van Rooijen C, Brouwers A, Chitnis AB, Peppelenbosch MP, Zivkovic D. d-Asb11 is an essential mediator of canonical delta-notch signalling. Nat Cell Biol. 2008;10:1190–8.

85 Da Silva MAS, Tee JM, Paridaen J, Brouwers A, Runtuwene V, Zivkovic D, Diks SH, Guardavaccaro D, Peppelenbosch MP. Essential role for the d-Asb11 cul5 box domain for proper notch signaling and neural cell fate decisions in vivo. PLoS One 2010;5.

86 Tee JM, da Silva MAS, Rygiel AM, Muncan V, Bink R, van den Brink GR, van Tijn P, Zivkovic D, Kodach LL, Guardavaccaro D, et al. asb11 is a regulator of embryonic and adult regenerative myogenesis. Stem Cells Dev. 2012;21:3091–103.

87 Bello NF, Lamsoul I, Heuzé ML, Métais A, Moreaux G, Calderwood DA, Duprez D, Moog-Lutz C, Lutz PG;The E3 ubiquitin ligase specificity subunit

ASB2beta is a novel regulator of muscle differentiation that targets filamin B to proteasomal degradation;Cell Death Differ. 2009 Jun;16(6):921-32. Epub 2009 Mar 20.

88 Guibal FC, Moog-Lutz C, Smolewski P, et al. ASB-2 inhibits growth and promotes commitment in myeloid leukemia cells. J Biol Chem.2002;277(1):218-224.

89 Bodine SC, Stitt TN, Gonzalez M, Kline WO, Stover GL, Bauerlein R, Zlotchenko E, Scrimgeour A, Lawrence JC, Glass DJ, Yancopoulus GD. Nat Cell Biol. 2001;3:1014–1019.

90 Gomes M.D., Lecker S.H., Jagoe R.T., Navon A., Goldberg A.L. Atrogin-1, a muscle-specific F-box protein highly expressed during muscle atrophy. Proceedings of the National Academy of Sciences of United States of America. 2001;98:14440–14445.

91 Milan G., Romanello V., Pescatore F., Armani A., Paik J.-H. H., Frasson L., et al. . (2015). Regulation of autophagy and the ubiquitin-proteasome system by the FoxO transcriptional network during muscle atrophy. Nat. Commun. 6:6670. 10.1038/ncomms7670

92 Sartori R., Schirwis E., Blaauw B., Bortolanza S., Zhao J., Enzo E., et al. . (2013). BMP signaling controls muscle mass. Nat. Genet. 45, 1309–1318. 10.1038/ng.2772

93 Stossel TP, Condeelis J, Cooley L, Hartwig JH, Noegel A, et al. Filamins as integrators of cell mechanics and signalling. Nat Rev Mol Cell Biol. 2001;2:138–145

94 Pudas R, Kiema TR, Butler PJ, Stewart M, Ylanne J. Structural basis for vertebrate filamin dimerization. Structure (Camb) 2005;13:111–119.

95 Hartwig JH, Tyler J, Stossel TP. Actin-binding protein promotes the bipolar and perpendicular branching of actin filaments. J Cell Biol. 1980;87:841–848.

96 Feng Y, Walsh CA. The many faces of filamin: a versatile molecular scaffold for cell motility and signalling. Nat Cell Biol. 2004;6:1034–1038

97 Popowicz GM, Schleicher M, Noegel AA, Holak TA. Filamins: promiscuous organizers of the cytoskeleton. Trends Biochem Sci. 2006;31:411–419

98 Davey JR1, Watt KI1, Parker BL2, Chaudhuri R2, Ryall JG3, Cunningham L1, Qian H1, Sartorelli V4, Sandri M5, Chamberlain J6, James DE7, Gregorevic P8.

Integrated expression analysis of muscle hypertrophy identifies Asb2 as a negative regulator of muscle mass. JCI Insight. 2016 Apr 21;1(5). pii: e85477.

99 Hirner S1, Krohne C, Schuster A, Hoffmann S, Witt S, Erber R, Sticht C, Gasch A, Labeit S, Labeit D. MuRF1-dependent regulation of systemic carbohydrate metabolism as revealed from transgenic mouse studies. J Mol Biol. 2008 Jun 13;379(4):666-77. doi: 10.1016/j.jmb.2008.03.049. Epub 2008 Apr 3.

100 Sartori R, Schirwis E, Blaauw B, Bortolanza S, Zhao J, Enzo E, Stantzou A, Mouisel E, Toniolo L, Ferry A, Stricker S, Goldberg AL, Dupont S, Piccolo S, Amthor H, Sandri M. Nat Genet. BMP signaling controls muscle mass.2013 Nov;45(11):1309-18. doi: 10.1038/ng.2772. Epub 2013 Sep 29.

101 Thottakara T1, Friedrich FW2, Reischmann S3, Braumann S3, Schlossarek S3, Krämer E3, Juhr D4, Schlüter H5, van der Velden J6, Münch J7, Patten M7, Eschenhagen T3, Moog-Lutz C8, Carrier L9. The E3 ubiquitin ligase Asb2β is downregulated in a mouse model of hypertrophic cardiomyopathy and targets desmin for proteasomal degradation. J Mol Cell Cardiol. 2015 Oct;87:214-24. doi: 10.1016/j.yjmcc.2015.08.020. Epub 2015 Sep 3

102 McCarthy JJ, Andrews JL, McDearmon EL, Campbell KS, Barber BK, Miller BH, et al. Identification of the Circadian Transcriptome in Adult Mouse Skeletal Muscle. Physiol Genomics. 2007;31:86–95.

103 Eckel-Mahan K1, Sassone-Corsi P. Epigenetic regulation of the molecular clockwork. Prog Mol Biol Transl Sci. 2013;119:29-50. doi: 10.1016/B978-0-12-396971-2.00002-6.

104 Bothe G. W., Haspel J. A., Smith C. L., Wiener H. H., Burden S. J. (2000). Selective

105 Smith and Barton: SMASH – semi-automatic muscle analysis using segmentation of histology: a MATLAB application. Received: 24 August 2014 Accepted: 15 October 2014 Published: 27 November 2014

106 Pfaffl M.W., Lange I.G., Daxenberger A., Meyer H.H. (2001). Tissue-specific expression pattern of estrogen receptors (ER): quantification of ER alpha and ER beta mRNA with real-time RT-PCR. APMIS. 109, 345-355